QCD Critical Point : Inching Towards Continuum

*Rajiv V. Gavai**

T. I. F. R., Mumbai, India

Introduction

Our Results on Critical Point

LQCD in Aid of Experiments

Summary

* *Work done with Saumen Datta & Sourendu Gupta, QM2012 proceedings & arXiv:1001.3796, 0806.2233.*

Critical Point : The eV Scale

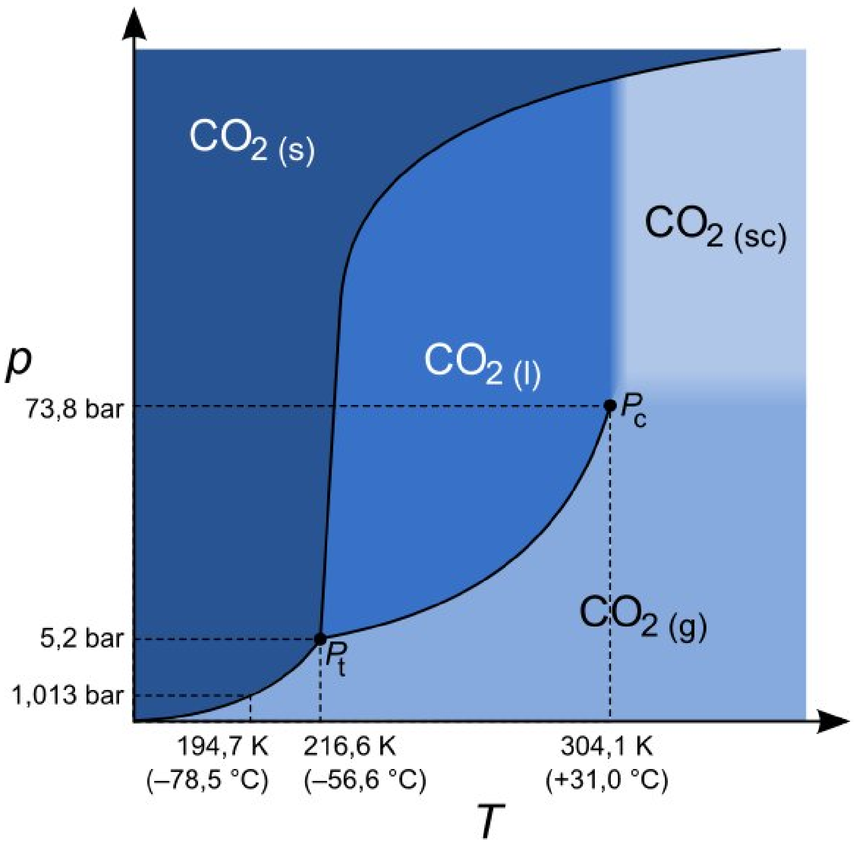

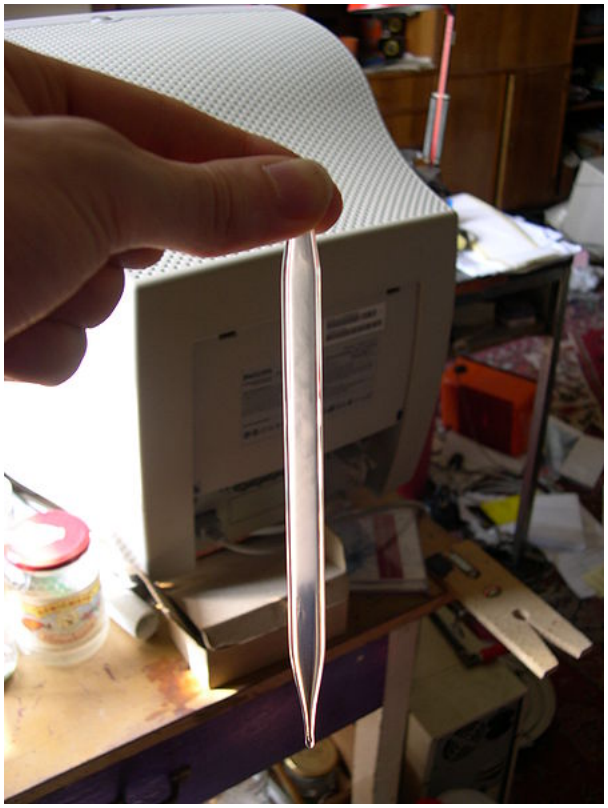

From Wikipedia

Introduction

♠ QCD Critical Point in T-μ_B plane – A fundamental aspect;

Introduction

♠ QCD Critical Point in T-μ_B plane – A fundamental aspect; Based on symmetries and models, the Expected QCD Phase Diagram

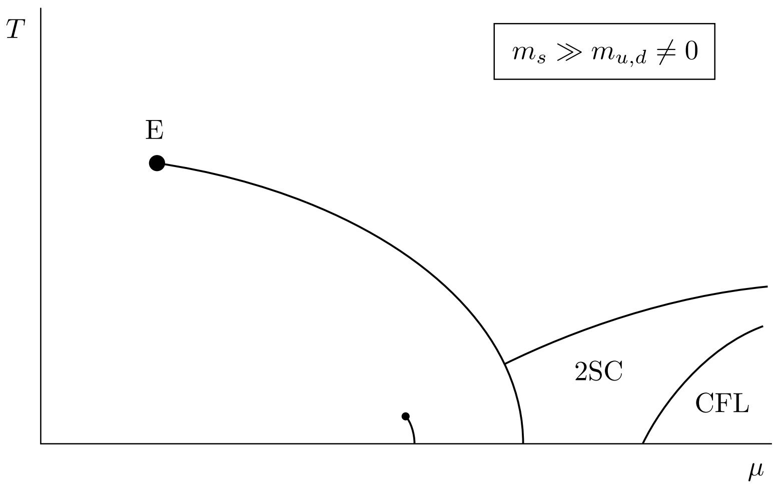

From Rajagopal-Wilczek Review

Introduction

♠ QCD Critical Point in T-μ_B plane – A fundamental aspect; Based on symmetries and models, the Expected QCD Phase Diagram

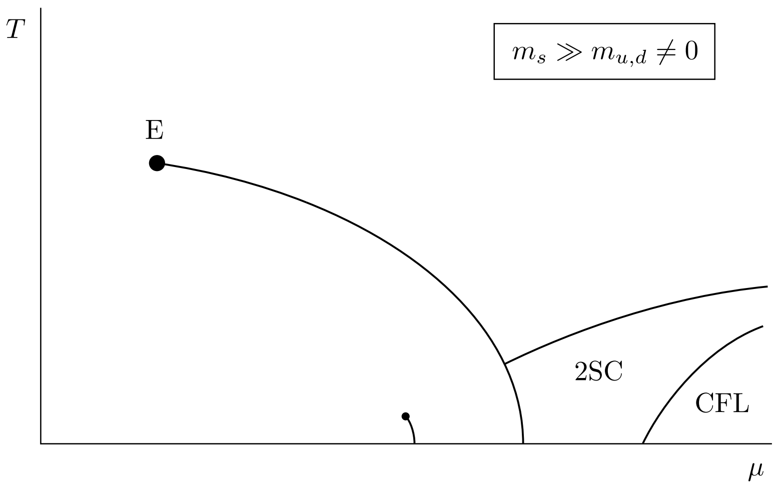

From Rajagopal-Wilczek Review

- Search for its location using *ab initio* methods
- Search for it in the experiments RHIC, FAIR,...

Introduction

♠ QCD Critical Point in T-μ_B plane – A fundamental aspect; Based on symmetries and models, the Expected QCD Phase Diagram

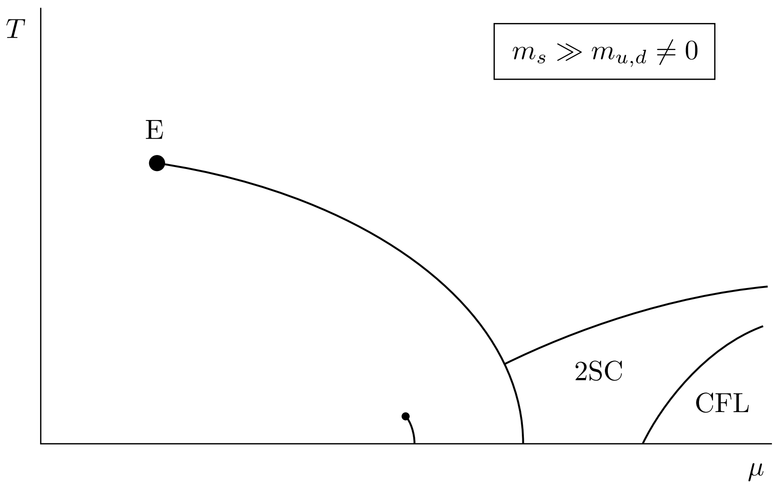

From Rajagopal-Wilczek Review

- Search for its location using *ab initio* methods
- Search for it in the experiments RHIC, FAIR,...
- What hints can Lattice QCD investigations provide ?

Why Lattice QCD ?

- Lattice QCD – Most Reliable and Completely parameter-free way to extract non-perturbative physics relevant to Heavy Ion Colliders.

- The Transition Temperature T_c, the Equation of State (used now in 'elliptic flow' analysis), and the Wróblewski Parameter λ_s etc. (Wuppertal-Budapest, HotQCD, GG '02)

Why Lattice QCD ?

- Lattice QCD – Most Reliable and Completely parameter-free way to extract non-perturbative physics relevant to Heavy Ion Colliders.

- The Transition Temperature T_c, the Equation of State (used now in 'elliptic flow' analysis), and the Wróblewski Parameter λ_s etc. (Wuppertal-Budapest, HotQCD, GG '02)

- Flavour Correlations (C_{BS}) and Charm Diffusion Coefficient D are some more such examples for RHIC Physics. (Gavai-Gupta, PRD 2006 & Banerjee et al. PRD 2012)

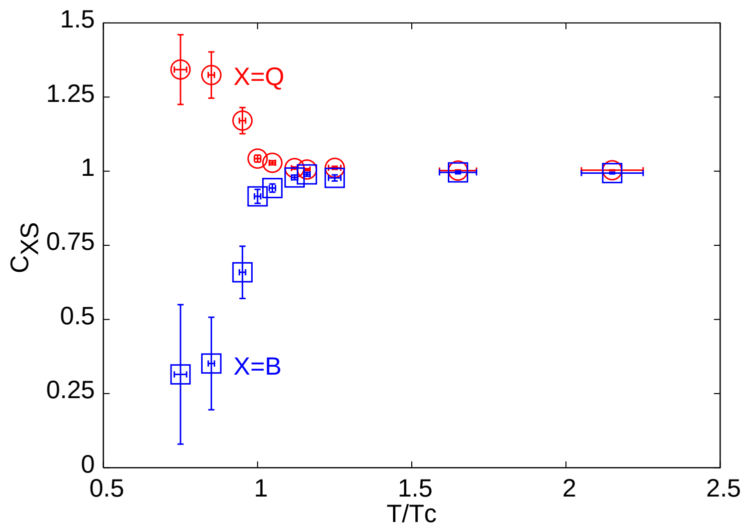

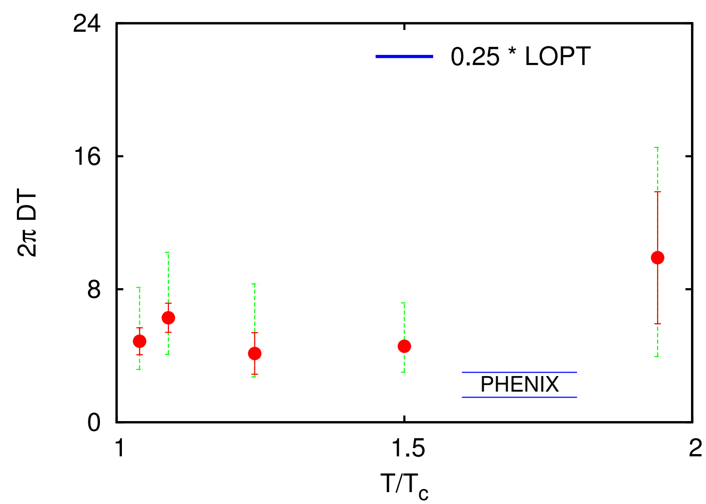

The $\mu \neq 0$ problem : Quark Type

- Mostly staggered quarks used in these simulations. Broken flavour and spin symmetry on lattice.

The $\mu \neq 0$ problem : Quark Type

- Mostly staggered quarks used in these simulations. Broken flavour and spin symmetry on lattice.

- Domain Wall or Overlap Fermions better. BUT Computationally expensive.

- Introduction of μ a la Bloch & Wettig (PRL 2006 & PRD2007)

The $\mu \neq 0$ problem : Quark Type

- Mostly staggered quarks used in these simulations. Broken flavour and spin symmetry on lattice.
- Domain Wall or Overlap Fermions better. BUT Computationally expensive.
- Introduction of μ a la Bloch & Wettig (PRL 2006 & PRD2007)
- Unfortunately breaks chiral symmetry ! (Banerjee, Gavai & Sharma PRD 2008; PoS (Lattice 2008); PRD 2009)
- Good News : Problem Solved !
  Overlap Lattice Action with exact chiral invariance at nonzero μ and any a now exists (Gavai & Sharma , arXiv : 1111.5944; PLB in press, Narayanan-Sharma JHEP '11).

The $\mu \neq 0$ problem : The Measure

Simulations can be done IF Det $M > 0$. However, det M is a complex number for any $\mu \neq 0$: The Phase/sign problem

The $\mu \neq 0$ problem : The Measure

Simulations can be done IF Det $M > 0$. However, det M is a complex number for any $\mu \neq 0$: The Phase/sign problem

Several Approaches proposed in the past two decades :

- Two parameter Re-weighting (Z. Fodor & S. Katz, JHEP 0203 (2002) 014).
- Imaginary Chemical Potential (Ph. de Forcrand & O. Philipsen, NP B642 (2002) 290; M.-P. Lombardo & M. D'Elia PR D67 (2003) 014505).
- Taylor Expansion (C. Allton et al., PR D68 (2003) 014507; R.V. Gavai and S. Gupta, PR D68 (2003) 034506).
- Canonical Ensemble (K. -F. Liu, IJMP B16 (2002) 2017, S. Kratochvila and P. de Forcrand, Pos LAT2005 (2006) 167.)
- Complex Langevin (G. Aarts and I. O. Stamatescu, arXiv:0809.5227 and its references for earlier work).

Why Taylor series expansion?

- Ease of taking continuum and thermodynamic limit.
- Better control of systematic errors.

Why Taylor series expansion?

- Ease of taking continuum and thermodynamic limit.
- Better control of systematic errors.
- E.g., $\exp[\Delta S]$ factor makes this exponentially tough for re-weighting.
- Discretization errors propagate in an unknown manner in re-weighting.

Why Taylor series expansion?

- Ease of taking continuum and thermodynamic limit.
- Better control of systematic errors.
- E.g., exp$[\Delta S]$ factor makes this exponentially tough for re-weighting.
- Discretization errors propagate in an unknown manner in re-weighting.

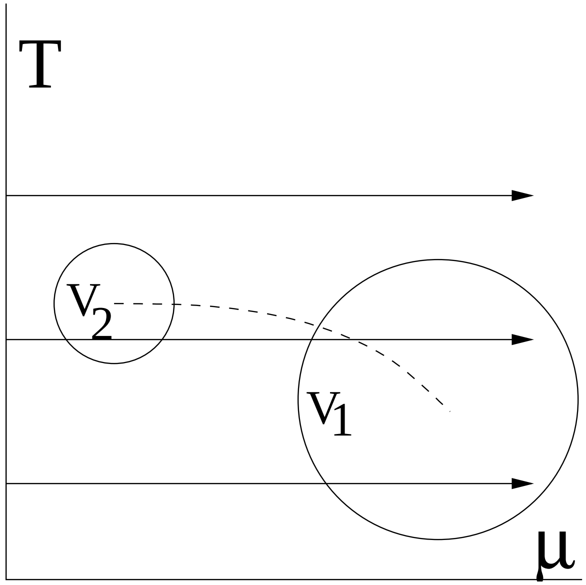

We studied volume dependence at several T to i) bracket the critical region and then ii) tracked its change as a function of volume.

Details of Expansion

Standard definitions yield various number densities and susceptibilities :

$$n_i = \frac{T}{V}\frac{\partial \ln \mathcal{Z}}{\partial \mu_i} \text{ and } \qquad \chi_{ij} = \frac{T}{V}\frac{\partial^2 \ln \mathcal{Z}}{\partial \mu_i \partial \mu_j} \quad .$$

These are also useful by themselves both theoretically and for Heavy Ion Physics (Flavour correlations, $\lambda_s \ldots$)

Denoting higher order susceptibilities by χ_{n_u,n_d}, the pressure P has the expansion in μ:

$$\frac{\Delta P}{T^4} \equiv \frac{P(\mu,T)}{T^4} - \frac{P(0,T)}{T^4} = \sum_{n_u,n_d} \chi_{n_u,n_d} \frac{1}{n_u!}\left(\frac{\mu_u}{T}\right)^{n_u} \frac{1}{n_d!}\left(\frac{\mu_d}{T}\right)^{n_d}$$

Details of Expansion

Standard definitions yield various number densities and susceptibilities :

$$n_i = \frac{T}{V}\frac{\partial \ln \mathcal{Z}}{\partial \mu_i} \text{ and } \qquad \chi_{ij} = \frac{T}{V}\frac{\partial^2 \ln \mathcal{Z}}{\partial \mu_i \partial \mu_j} \quad .$$

These are also useful by themselves both theoretically and for Heavy Ion Physics (Flavour correlations, $\lambda_s \ldots$)

Denoting higher order susceptibilities by χ_{n_u,n_d}, the pressure P has the expansion in μ:

$$\frac{\Delta P}{T^4} \equiv \frac{P(\mu,T)}{T^4} - \frac{P(0,T)}{T^4} = \sum_{n_u,n_d} \chi_{n_u,n_d} \frac{1}{n_u!} \left(\frac{\mu_u}{T}\right)^{n_u} \frac{1}{n_d!} \left(\frac{\mu_d}{T}\right)^{n_d}$$

- From this expansion, a series for baryonic susceptibility can be constructed. Its radius of convergence gives estimate of the location of nearest critical point.

- Successive estimates for the radius of convergence obtained from these using $\sqrt{\frac{n(n+1)\chi_B^{(n+1)}}{\chi_B^{(n+3)}T^2}}$ or $\left(n!\frac{\chi_B^{(2)}}{\chi_B^{(n+2)}T^2}\right)^{1/n}$. We use both and terms up to 8th order in μ.

- All coefficients of the series must be POSITIVE for the critical point to be at real μ, and thus physical.

- We (Gavai-Gupta '05, '09) use up to 8^{th} order. B-RBC so far has up to 6^{th} order.

- 10th & even 12th order may be possible : Ideas to extend to higher orders are emerging (Gavai-Sharma PRD 2012 & PRD 2010) which save up to 60 % computer time.

- From this expansion, a series for baryonic susceptibility can be constructed. Its radius of convergence gives estimate of the location of nearest critical point.

- Successive estimates for the radius of convergence obtained from these using $\sqrt{\frac{n(n+1)\chi_B^{(n+1)}}{\chi_B^{(n+3)}T^2}}$ or $\left(n!\frac{\chi_B^{(2)}}{\chi_B^{(n+2)}T^2}\right)^{1/n}$. We use both and terms up to 8th order in μ.

- All coefficients of the series must be POSITIVE for the critical point to be at real μ, and thus physical.

- We (Gavai-Gupta '05, '09) use up to 8^{th} order. B-RBC so far has up to 6^{th} order.

- 10th & even 12th order may be possible : Ideas to extend to higher orders are emerging (Gavai-Sharma PRD 2012 & PRD 2010) which save up to 60 % computer time.

- From this expansion, a series for baryonic susceptibility can be constructed. Its radius of convergence gives estimate of the location of nearest critical point.
- Successive estimates for the radius of convergence obtained from these using $\sqrt{\frac{n(n+1)\chi_B^{(n+1)}}{\chi_B^{(n+3)}T^2}}$ or $\left(n!\frac{\chi_B^{(2)}}{\chi_B^{(n+2)}T^2}\right)^{1/n}$. We use both and terms up to 8th order in μ.
- All coefficients of the series must be POSITIVE for the critical point to be at real μ, and thus physical.
- We (Gavai-Gupta '05, '09) use up to 8^{th} order. B-RBC so far has up to 6^{th} order.
- 10th & even 12th order may be possible : Ideas to extend to higher orders are emerging (Gavai-Sharma PRD 2012 & PRD 2010) which save up to 60 % computer time.

The Susceptibilities

All susceptibilities can be written as traces of products of M^{-1} and various derivatives of M.

At leading order,

$$\chi_{20} = \frac{T}{V}[\langle \mathcal{O}_2 + \mathcal{O}_{11} \rangle], \qquad \chi_{11} = \frac{T}{V}[\langle \mathcal{O}_{11} \rangle]$$

Here $\mathcal{O}_2 = \mathrm{Tr}\ M^{-1}M'' - \mathrm{Tr}\ M^{-1}M'M^{-1}M'$, and $\mathcal{O}_{11} = (\mathrm{Tr}\ M^{-1}M')^2$. The traces are estimated by a stochastic method (Gottlieb et al., PRL '87):
$\mathrm{Tr}\ A = \sum_{i=1}^{N_v} R_i^\dagger A R_i / 2N_v$, and $(\mathrm{Tr}\ A)^2 = 2 \sum_{i>j=1}^{L} (\mathrm{Tr}\ A)_i (\mathrm{Tr}\ A)_j / L(L-1)$, where R_i is a complex vector from a set of N_v subdivided in L independent sets.

The Susceptibilities

All susceptibilities can be written as traces of products of M^{-1} and various derivatives of M.

At leading order,

$$\chi_{20} = \frac{T}{V}[\langle \mathcal{O}_2 + \mathcal{O}_{11} \rangle], \qquad \chi_{11} = \frac{T}{V}[\langle \mathcal{O}_{11} \rangle]$$

Here $\mathcal{O}_2 = \mathrm{Tr}\ M^{-1}M'' - \mathrm{Tr}\ M^{-1}M'M^{-1}M'$, and $\mathcal{O}_{11} = (\mathrm{Tr}\ M^{-1}M')^2$. The traces are estimated by a stochastic method (Gottlieb et al., PRL '87):
$\mathrm{Tr}\ A = \sum_{i=1}^{N_v} R_i^\dagger A R_i / 2N_v$, and $(\mathrm{Tr}\ A)^2 = 2\sum_{i>j=1}^{L} (\mathrm{Tr}\ A)_i (\mathrm{Tr}\ A)_j / L(L-1)$, where R_i is a complex vector from a set of N_v subdivided in L independent sets.

Higher order NLS are more involved. E.g.,

$$\chi_{40} = \frac{T}{V}\left[\left\langle \mathcal{O}_{1111} + 6\mathcal{O}_{112} + 4\mathcal{O}_{13} + 3\mathcal{O}_{22} + \mathcal{O}_4 \right\rangle - 3\left\langle \mathcal{O}_{11} + \mathcal{O}_2 \right\rangle^2\right].$$

Here the notation $\mathcal{O}_{ij\ldots l}$ stands for the product, $\mathcal{O}_i\mathcal{O}_j \cdots O_l$ and
$\mathcal{O}_3 = 2\ \mathrm{Tr}\ (M^{-1}M')^3 - 3\ \mathrm{Tr}\ M^{-1}M'M^{-1}M'' + \mathrm{Tr}\ M^{-1}M'''$,
$\mathcal{O}_4 = -6\ \mathrm{Tr}\ (M^{-1}M')^4 + 12\ \mathrm{Tr}\ (M^{-1}M')^2M^{-1}M'' - 3\ \mathrm{Tr}\ (M^{-1}M'')^2 -$
$3\ \mathrm{Tr}\ M^{-1}M'M^{-1}M''' + \mathrm{Tr}\ M^{-1}M''''$.

At the 8th order, terms involve operators up to $\mathcal{O}_8$ which in turn have terms up to 8 quark propagators and combinations of M' and M''. In fact, the entire evaluation of the χ_{80} needs 20 inversions of Dirac matrix.

This can be reduced to 8 inversions using an action linear in μ (Gavai-Sharma PRD 2012 & PRD 2010), leading still to results in agreement with that exponential in μ.

Higher order NLS are more involved. E.g.,

$$\chi_{40} = \frac{T}{V}\left[\left\langle \mathcal{O}_{1111} + 6\mathcal{O}_{112} + 4\mathcal{O}_{13} + 3\mathcal{O}_{22} + \mathcal{O}_4 \right\rangle - 3\left\langle \mathcal{O}_{11} + \mathcal{O}_2 \right\rangle^2\right].$$

Here the notation $\mathcal{O}_{ij\ldots l}$ stands for the product, $\mathcal{O}_i\mathcal{O}_j \cdots O_l$ and
$\mathcal{O}_3 = 2 \text{ Tr } (M^{-1}M')^3 - 3 \text{ Tr } M^{-1}M'M^{-1}M'' + \text{Tr } M^{-1}M'''$,
$\mathcal{O}_4 = -6 \text{ Tr } (M^{-1}M')^4 + 12 \text{ Tr } (M^{-1}M')^2M^{-1}M'' - 3 \text{ Tr } (M^{-1}M'')^2 -$
$3 \text{ Tr } M^{-1}M'M^{-1}M''' + \text{Tr } M^{-1}M''''$.

At the 8th order, terms involve operators up to $\mathcal{O}_8$ which in turn have terms up to 8 quark propagators and combinations of M' and M''. In fact, the entire evaluation of the χ_{80} needs 20 inversions of Dirac matrix.

This can be reduced to 8 inversions using an action linear in μ (Gavai-Sharma PRD 2012 & PRD 2010), leading still to results in agreement with that exponential in μ.

Our Simulations & Results

- Staggered fermions with $N_f = 2$ of $m/T_c = 0.1$; R-algorithm used.
- $m_\pi/m_\rho = 0.31 \pm 0.01$ (MILC); Kept the same as $a \to 0$ (on all N_t).
- Earlier Lattice : 4 $\times N_s^3$, $N_s =$ 8, 10, 12, 16, 24 (Gavai-Gupta, PRD 2005)
  Finer Lattice : 6 $\times N_s^3$, $N_s =$ 12, 18, 24 (Gavai-Gupta, PRD 2009).

Our Simulations & Results

- Staggered fermions with $N_f = 2$ of $m/T_c = 0.1$; R-algorithm used.
- $m_\pi/m_\rho = 0.31 \pm 0.01$ (MILC); Kept the same as $a \to 0$ (on all N_t).
- Earlier Lattice : 4 $\times N_s^3$, N_s = 8, 10, 12, 16, 24 (Gavai-Gupta, PRD 2005)
  Finer Lattice : 6 $\times N_s^3$, N_s = 12, 18, 24 (Gavai-Gupta, PRD 2009).
- Even finer Lattice : 8 $\times 32^3$ — This Talk (Datta-RVG-Gupta, '12)
  Aspect ratio, N_s/N_t, maintained four to reduce finite volume effects.
- Simulations made at T/T_c = 0.90, 0.92, 0.94, 0.96, 0.98, 1.00, 1.02, 1.12, 1.5 and 2.01. Typical stat. 100-200 in max autocorrelation units.
- T_c — defined by the peak of Polyakov loop susceptibility.

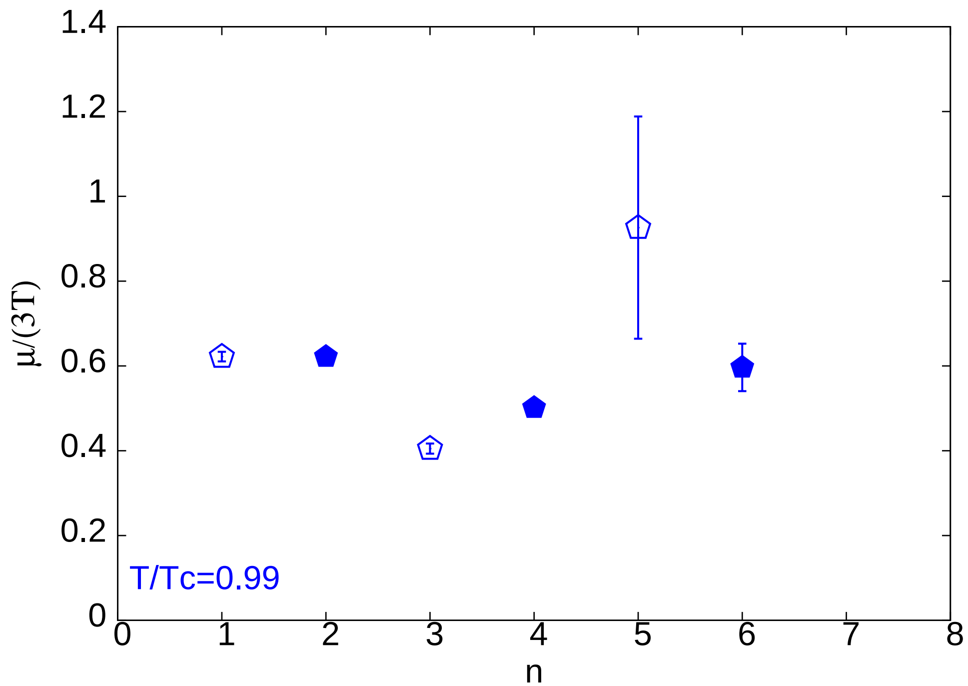

1.4
1.2
1
0.8
0.6
0.4
0.2
0
μ/(3T)
T/Tc=0.99
0 1 2 3 4 5 6 7 8
n

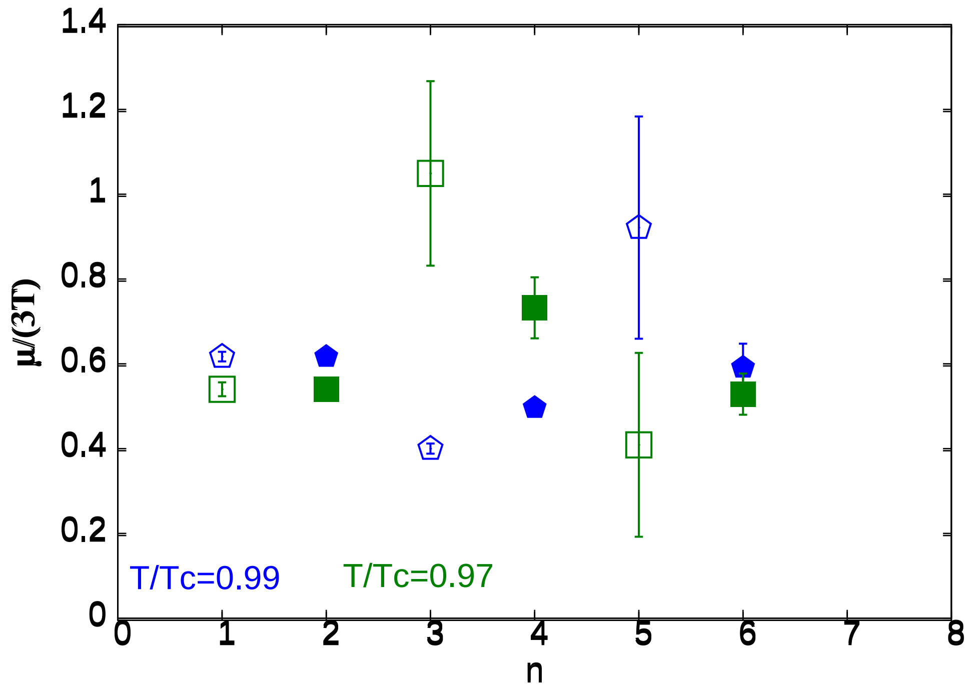
1.4
1.2
1
0.8
0.6
0.4
0.2
0
μ/(3T)
0
1
2
3
4
5
6
7
8
n
T/Tc=0.99
T/Tc=0.97

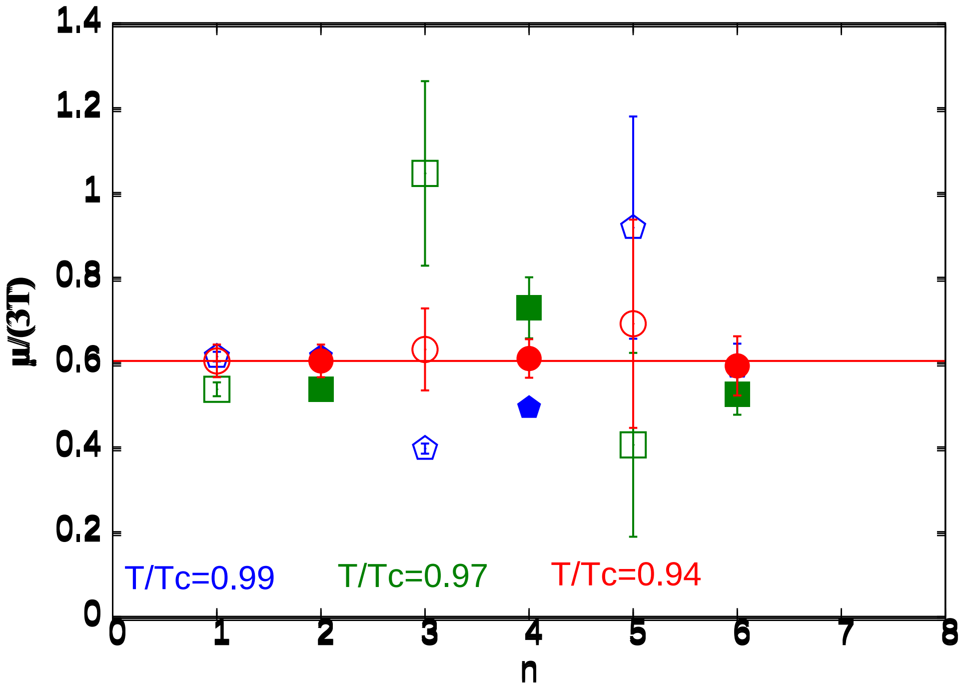
μ/(3T)
n
T/Tc=0.99
T/Tc=0.97
T/Tc=0.94

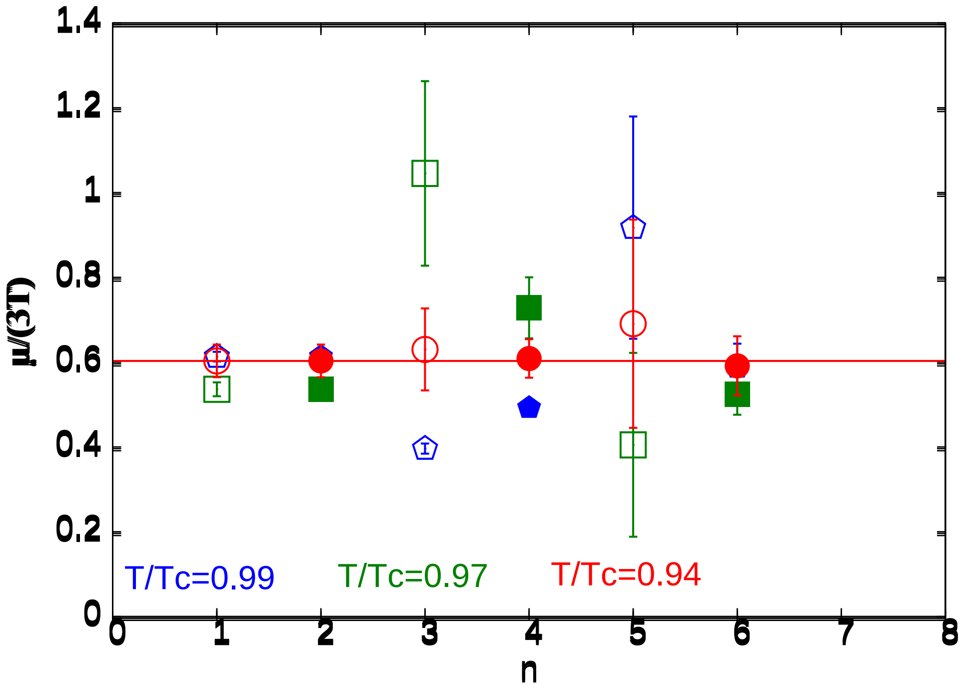

- $\frac{T^E}{T_c} = 0.94 \pm 0.01$, and $\frac{\mu_B^E}{T^E} = 1.8 \pm 0.1$ for finer lattice: Our earlier coarser lattice result was $\mu_B^E/T^E = 1.3 \pm 0.3$. Infinite volume result: $\downarrow$ to 1.1(1)

- Critical point at $\mu_B/T \sim 1 - 2$.

Cross Check on μ^E/T^E

♠ Use the series directly to construct χ_B for nonzero μ $\longrightarrow$ smooth curves with no signs of criticality.

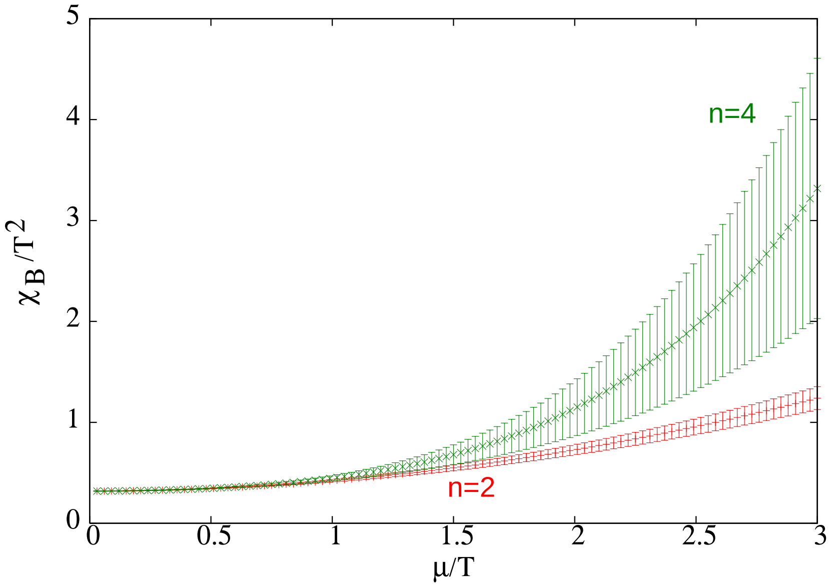

Cross Check on μ^E/T^E

♠ Use the series directly to construct χ_B for nonzero $\mu \longrightarrow$ smooth curves with no signs of criticality.

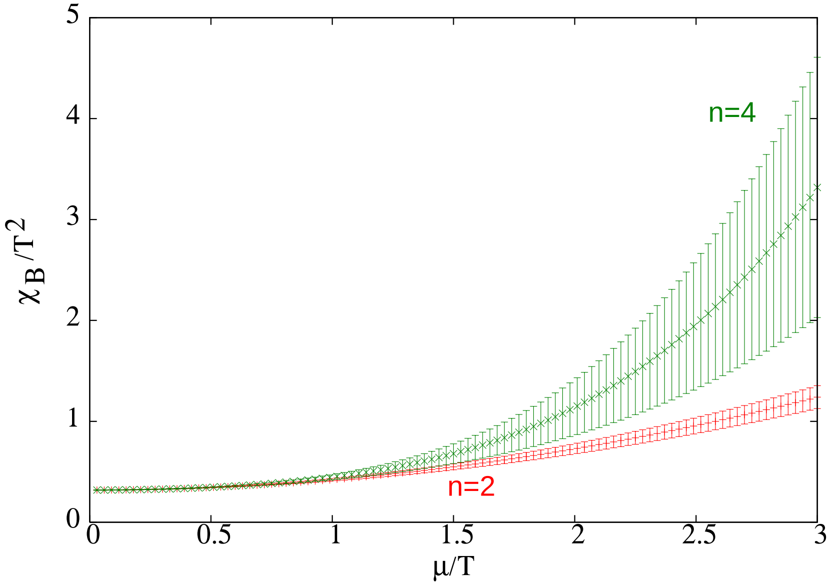

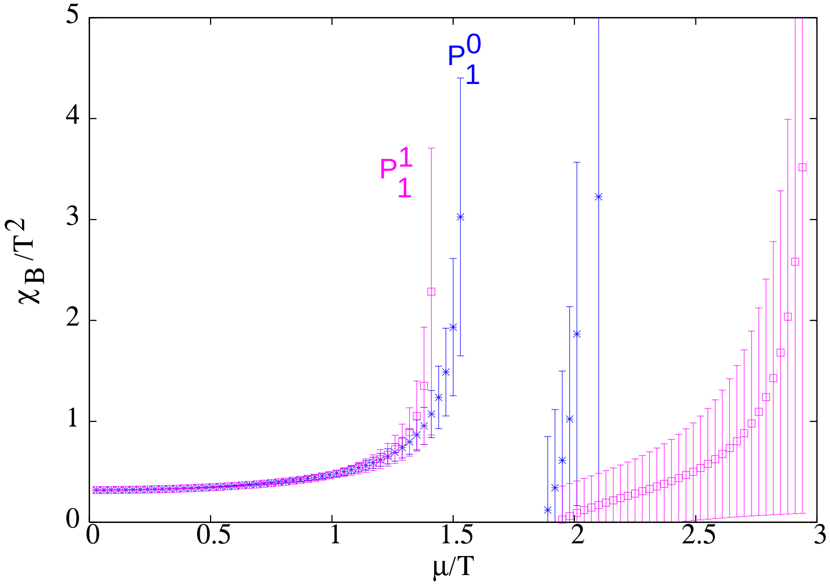

♠ Use Padé approximants for the series to estimate the radius of convergence.

♡ Consistent Window with our other estimates.

Critical Point : Story thus far

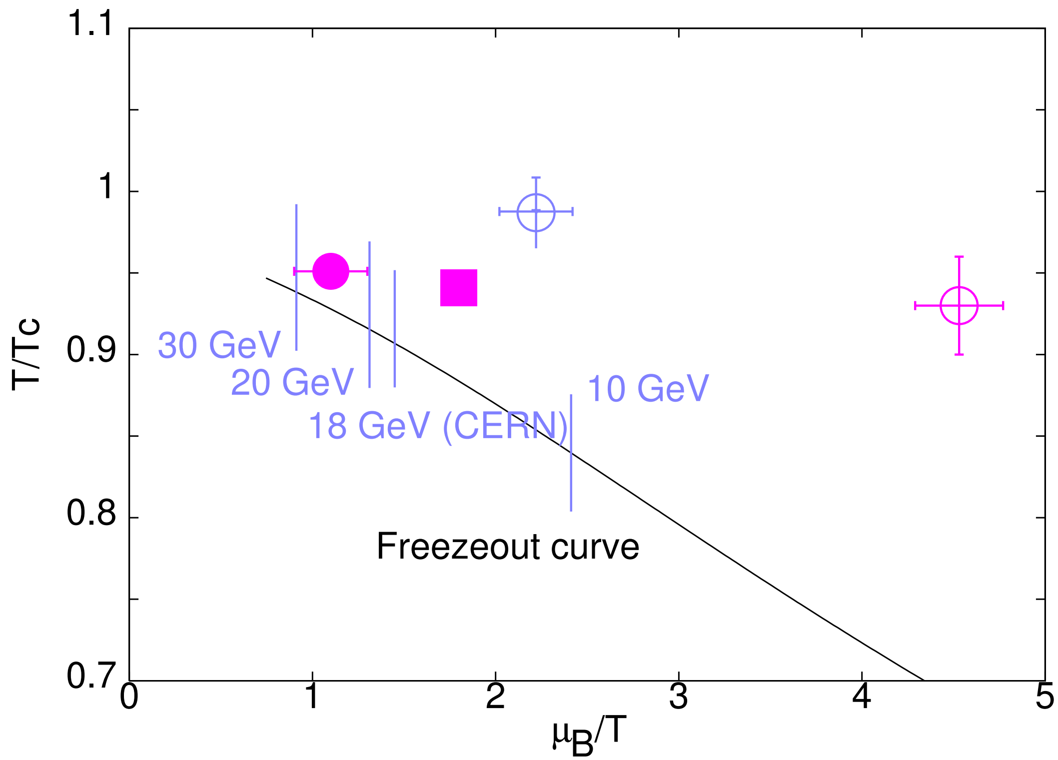

♠ $N_f = 2$ (magenta) and 2+1 (blue) (Fodor-Katz, JHEP '04).

♡ $N_t = 4$ Circles (GG '05 & Fodor-Katz JHEP '02), $N_t = 6$ Box (GG '09).

χ_2 for $N_t = 8$, 6, and 4 lattices

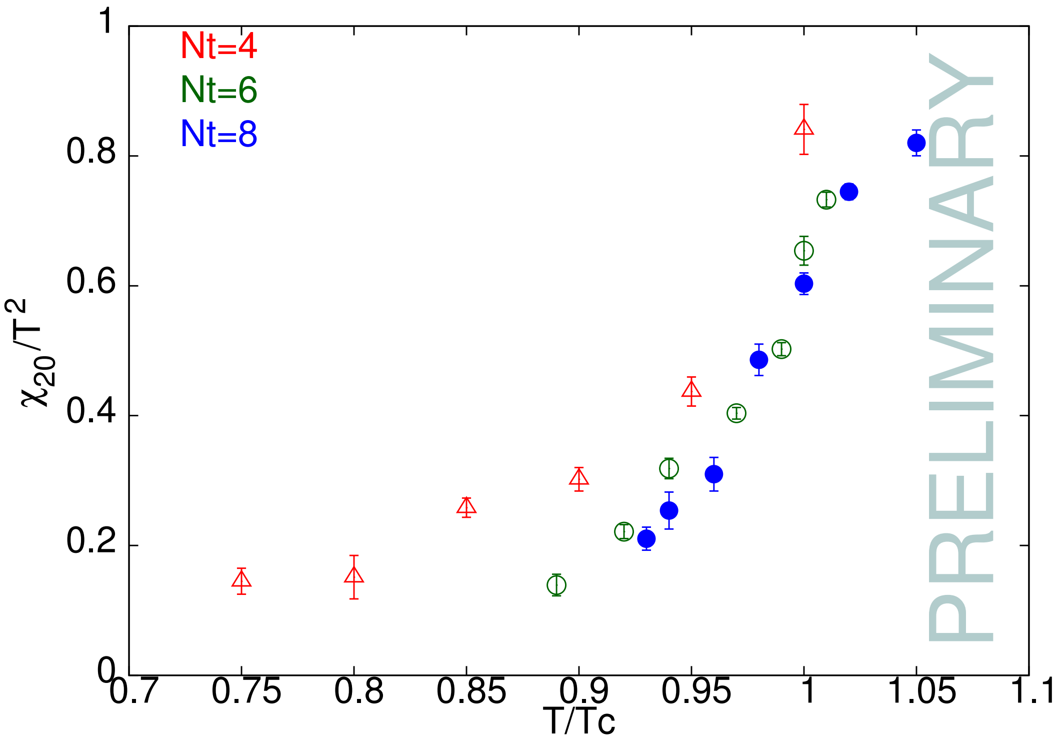

♠ $N_t = 8$ (Datta-Gavai-Gupta, QM12) and 6 (GG, PRD '09) results agree.

♡ $\beta_c(N_t = 8)$ agrees with Gottlieb et al. PR D47,1993.

Radius of Convergence result

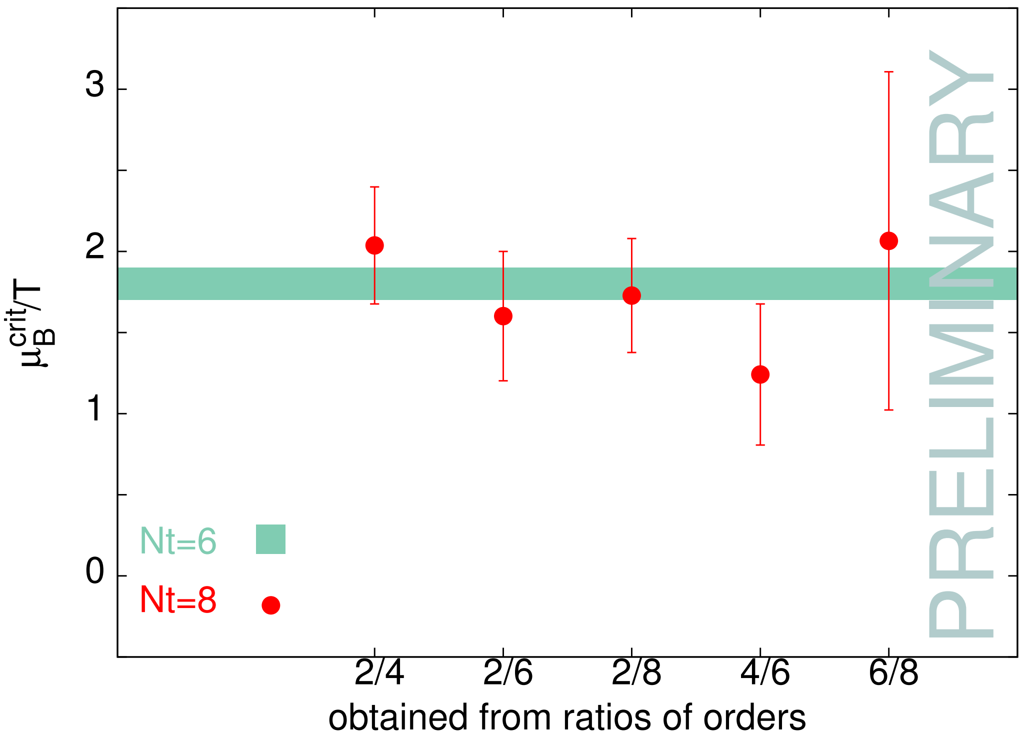

♠ At our (T_E, μ_E) for $N_t = 6$, the ratios display constancy for $N_t = 8$ as well.

♡ Currently : Similar results at neighbouring $T/T_c \Longrightarrow$ a larger ΔT at same μ_B^E.

Critical Point : Inching Towards Continuum

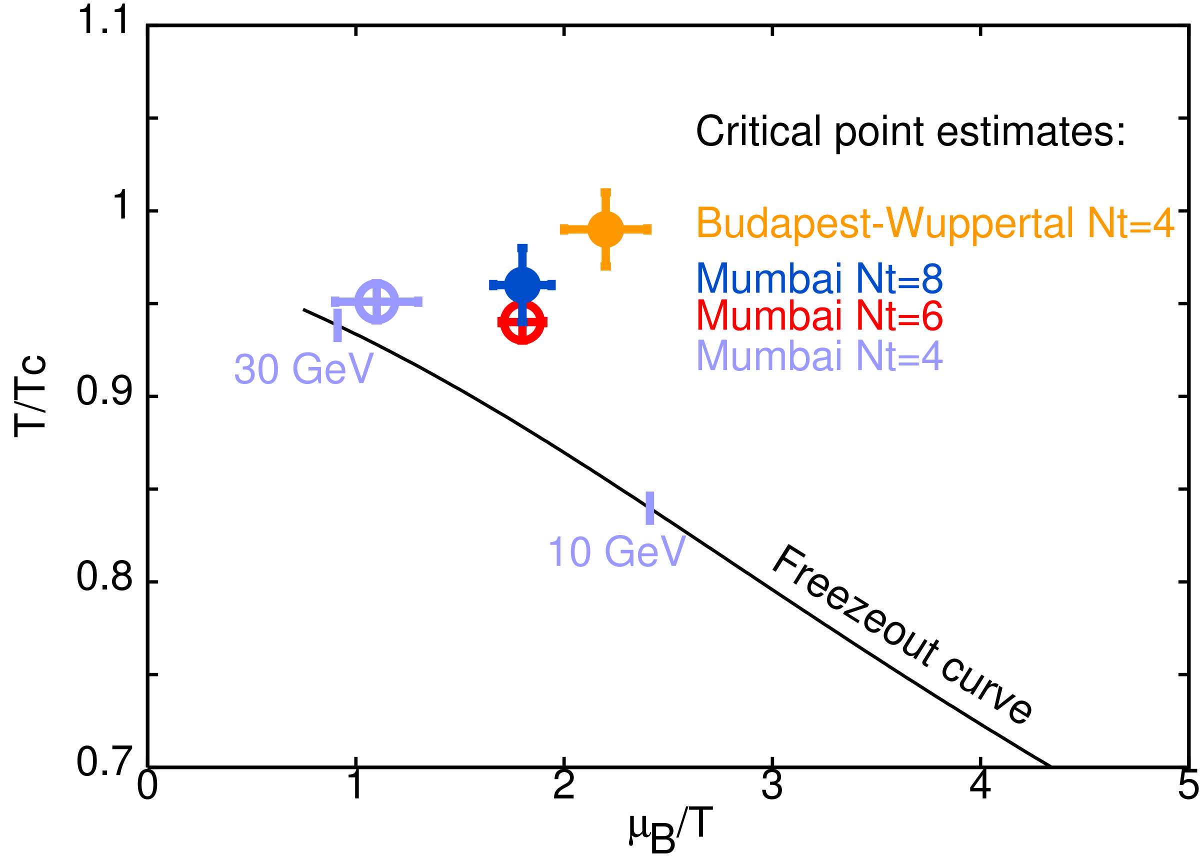

Lattice predictions along the freezeout curve

- Hadron yields well described using Statistical Models, leading to a freezeout curve in the T-μ_B plane. (Andronic, Braun-Munzinger & Stachel, PLB 2009 ; Oeschler, Cleymans, Redlich & Wheaton, 2009)

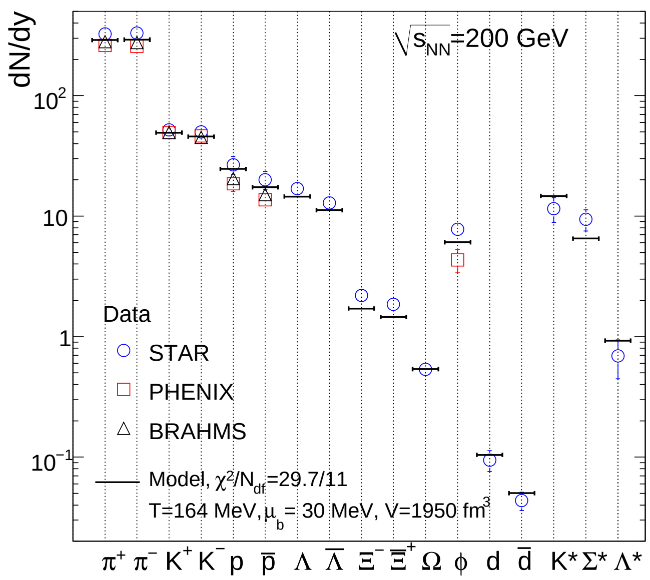

Lattice predictions along the freezeout curve

- Hadron yields well described using Statistical Models, leading to a freezeout curve in the T-μ_B plane. (Andronic, Braun-Munzinger & Stachel, PLB 2009 ; Oeschler, Cleymans, Redlich & Wheaton, 2009)

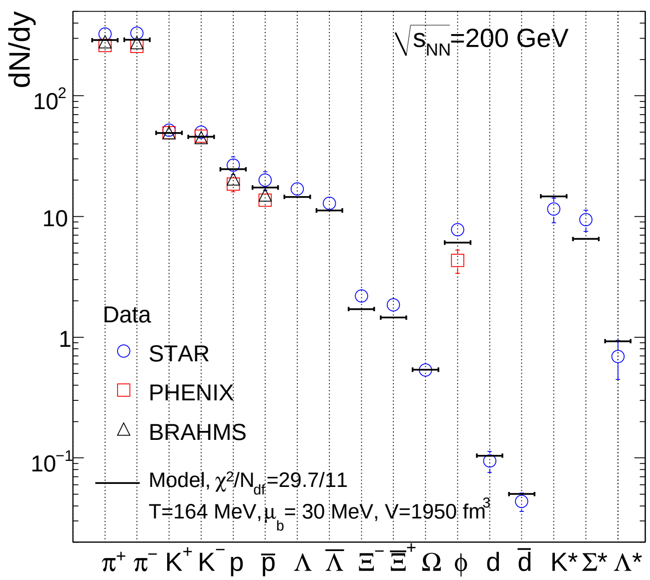

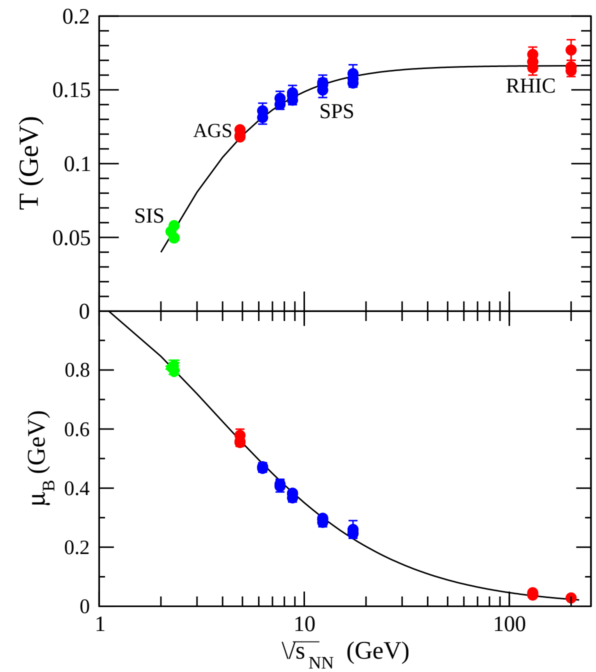

- Plotting these results in the T-μ_B plane, one has the freezeout curve, which was shown to correspond the $\langle E\rangle/\langle N\rangle \simeq 1$. (Cleymans and Redlich, PRL 1998)

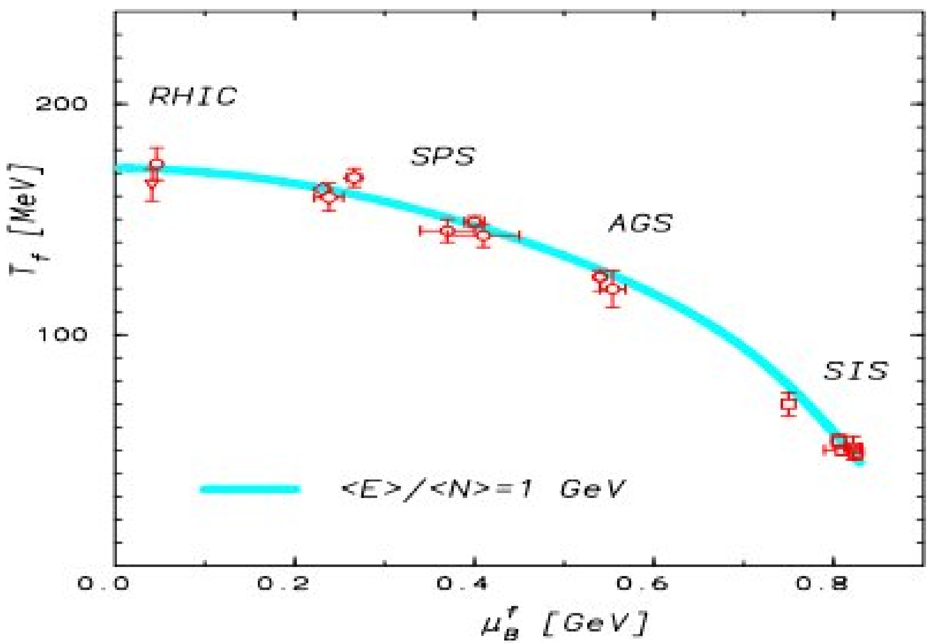

(From Braun-Munzinger, Redlich and Stachel nucl-th/0304013)

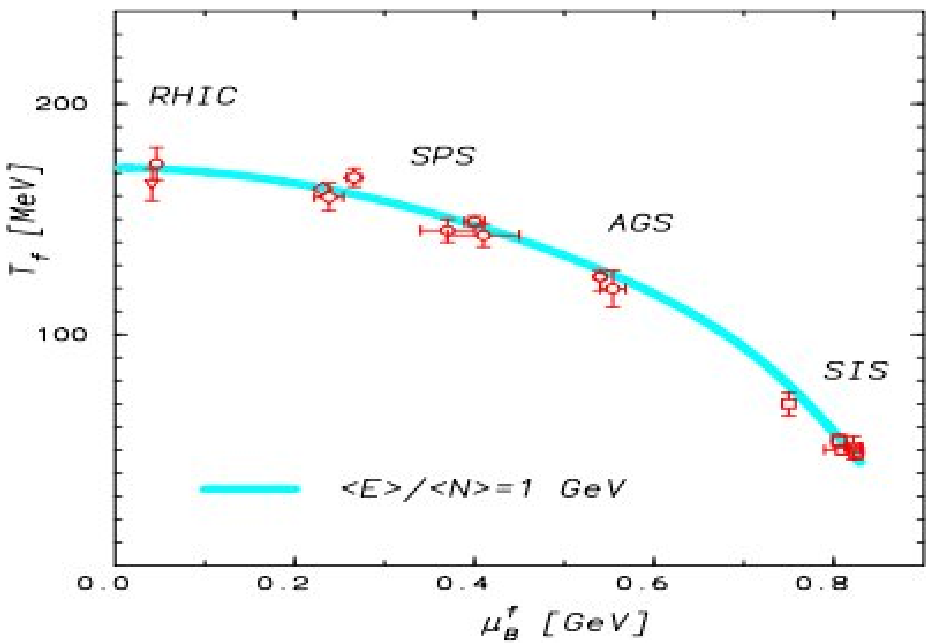

(From Braun-Munzinger, Redlich and Stachel nucl-th/0304013)

- Note : Freeze-out curve is based soled on data on hadron yields, & gives the (T, μ) accessible in heavy-ion experiments.

- Our Key Proposal : Use the freezeout curve from hadron abundances to *predict* fluctuations using lattice QCD along it. (Gavai-Gupta, TIFR/TH/10-01, arXiv 1001.3796)

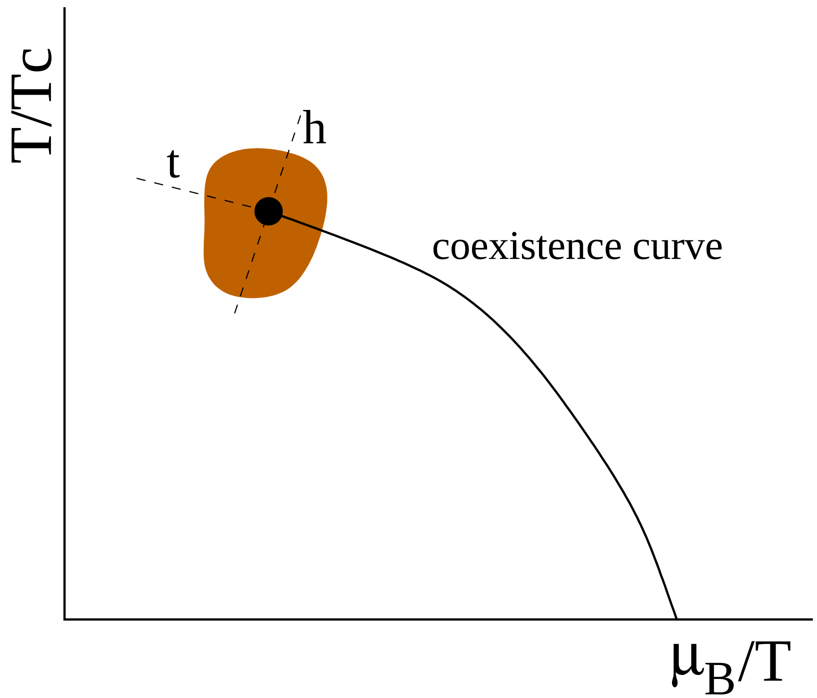
T/Tc
h
t
coexistence curve
μ_B/T

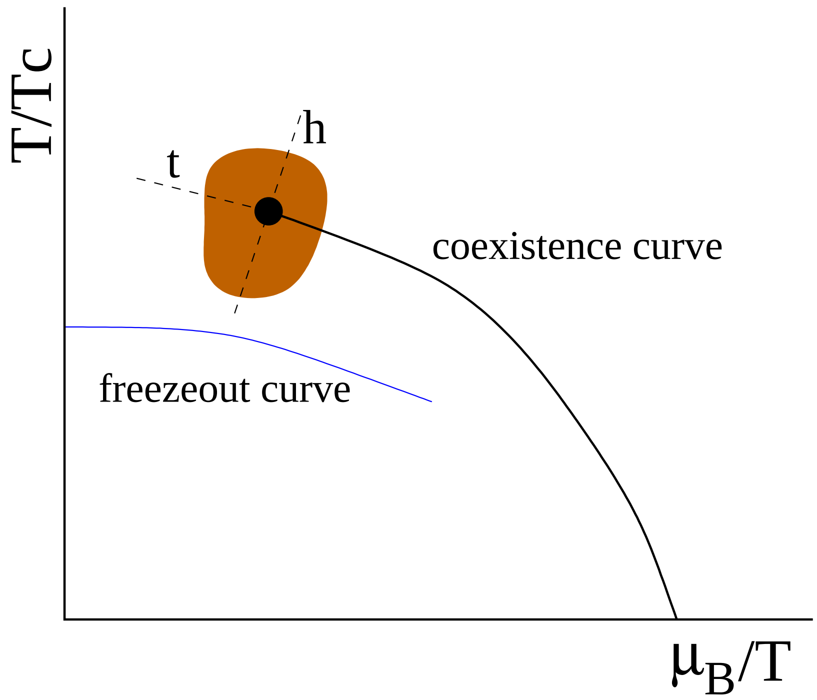
T/Tc
h
t
coexistence curve
freezeout curve
μB/T

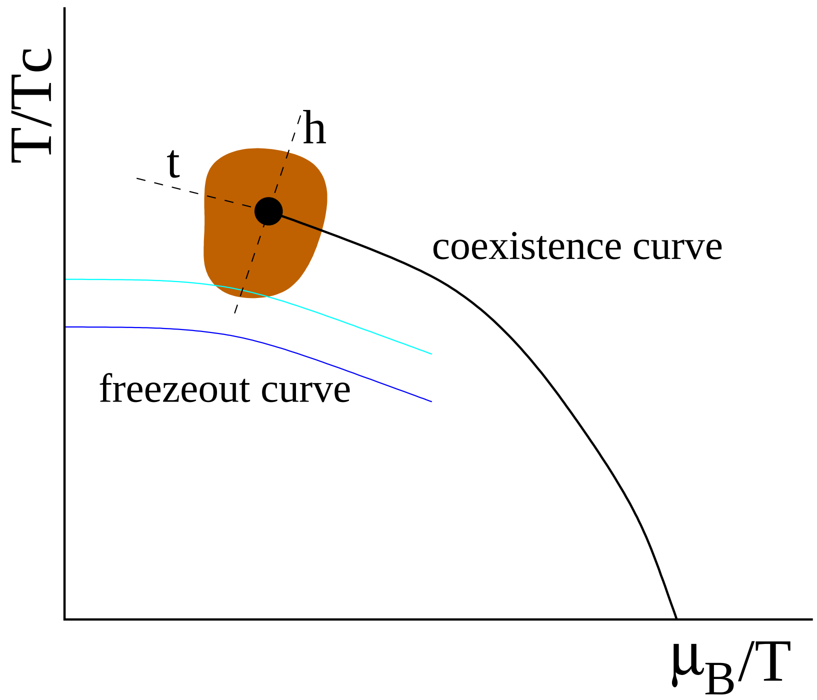
T/Tc
h
t
coexistence curve
freezeout curve
μB/T

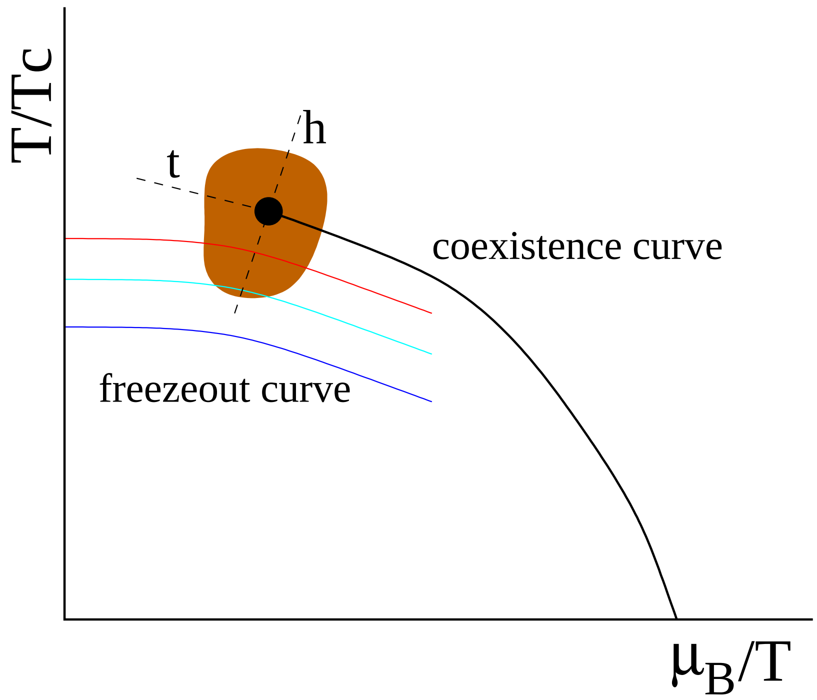
T/Tc
h
t
coexistence curve
freezeout curve
μ_B/T

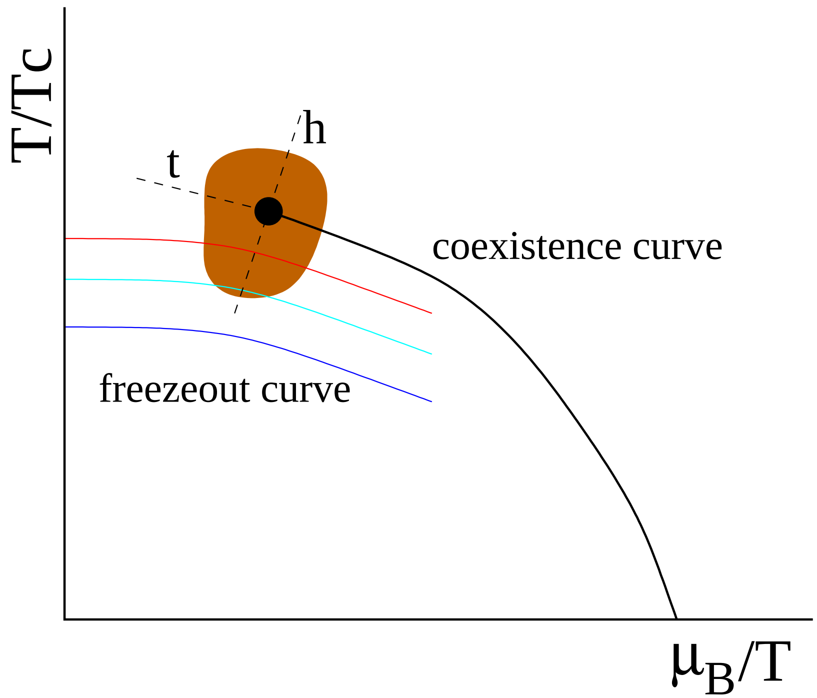

- Use the freezeout curve to relate $(T, \mu_B)$to $\sqrt{s}$ and employ lattice QCD predictions along it. (Gavai-Gupta, TIFR/TH/10-01, arXiv 1001.3796)

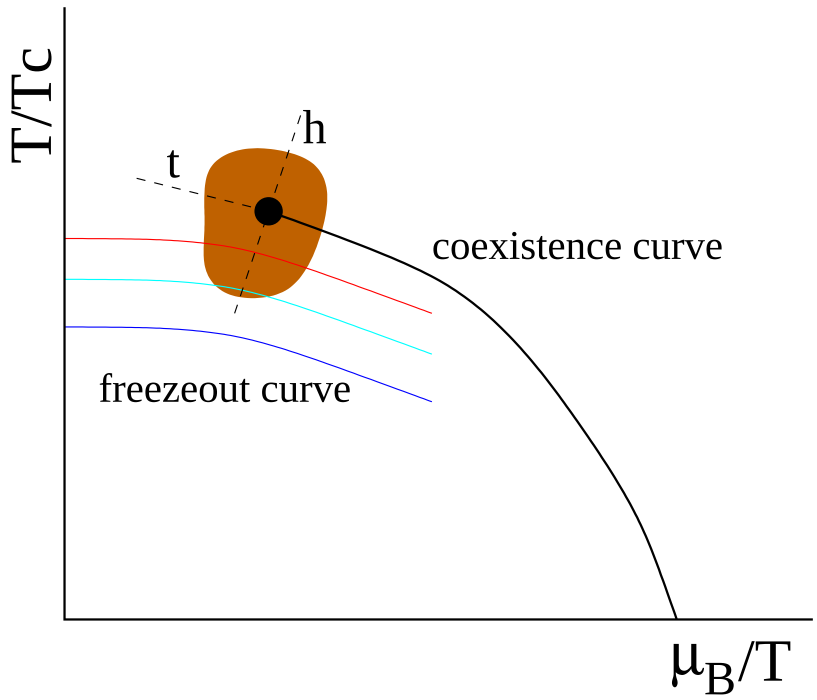

- Use the freezeout curve to relate $(T, \mu_B)$to $\sqrt{s}$ and employ lattice QCD predictions along it. (Gavai-Gupta, TIFR/TH/10-01, arXiv 1001.3796)

- Define $m_1 = \frac{T\chi^{(3)}(T,\mu_B)}{\chi^{(2)}(T,\mu_B)}$, $m_3 = \frac{T\chi^{(4)}(T,\mu_B)}{\chi^{(3)}(T,\mu_B)}$, and $m_2 = m_1 m_3$ and use the Padè method to construct them.

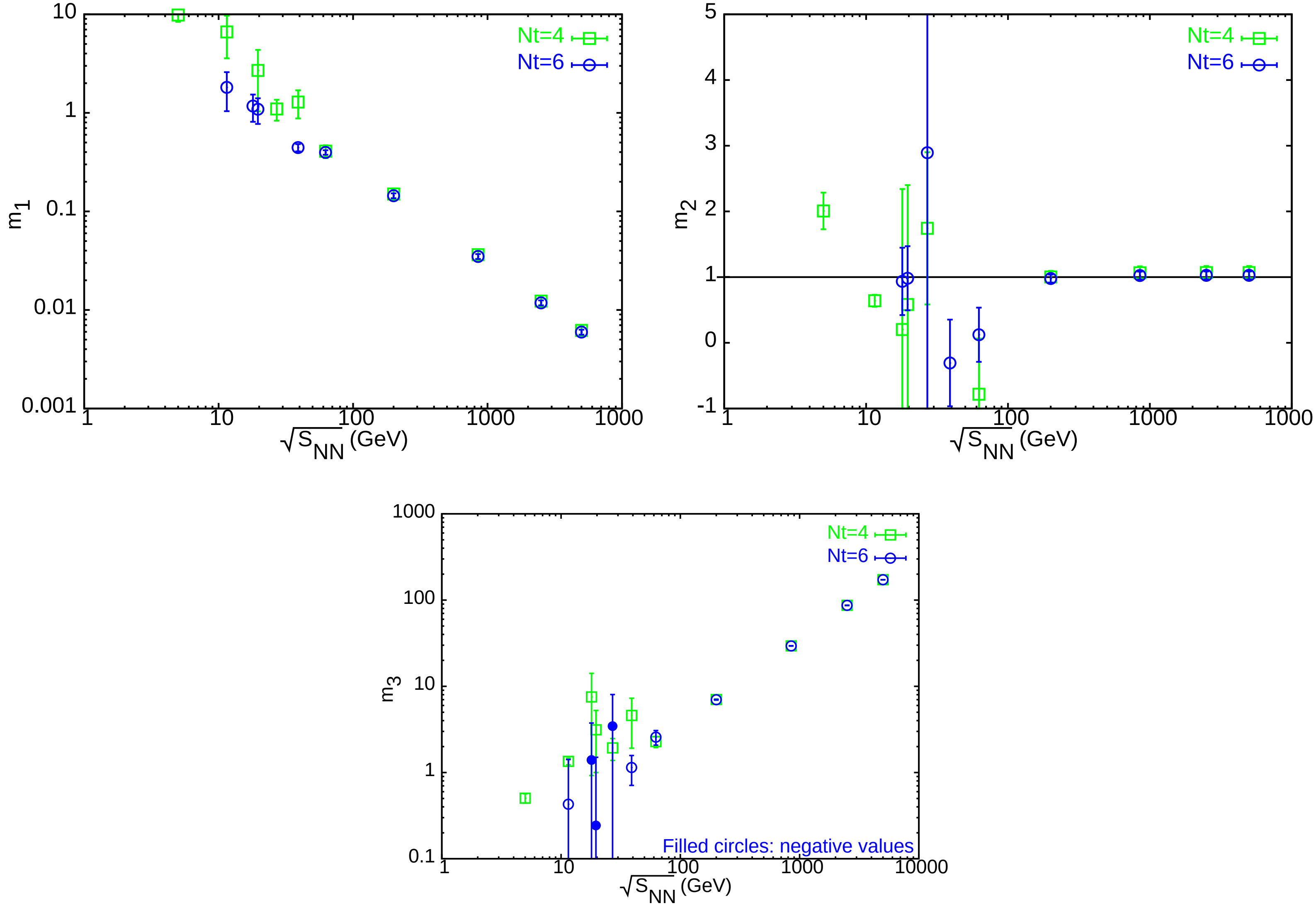

♠ Gavai & Gupta, arXiv: 1001.3796.

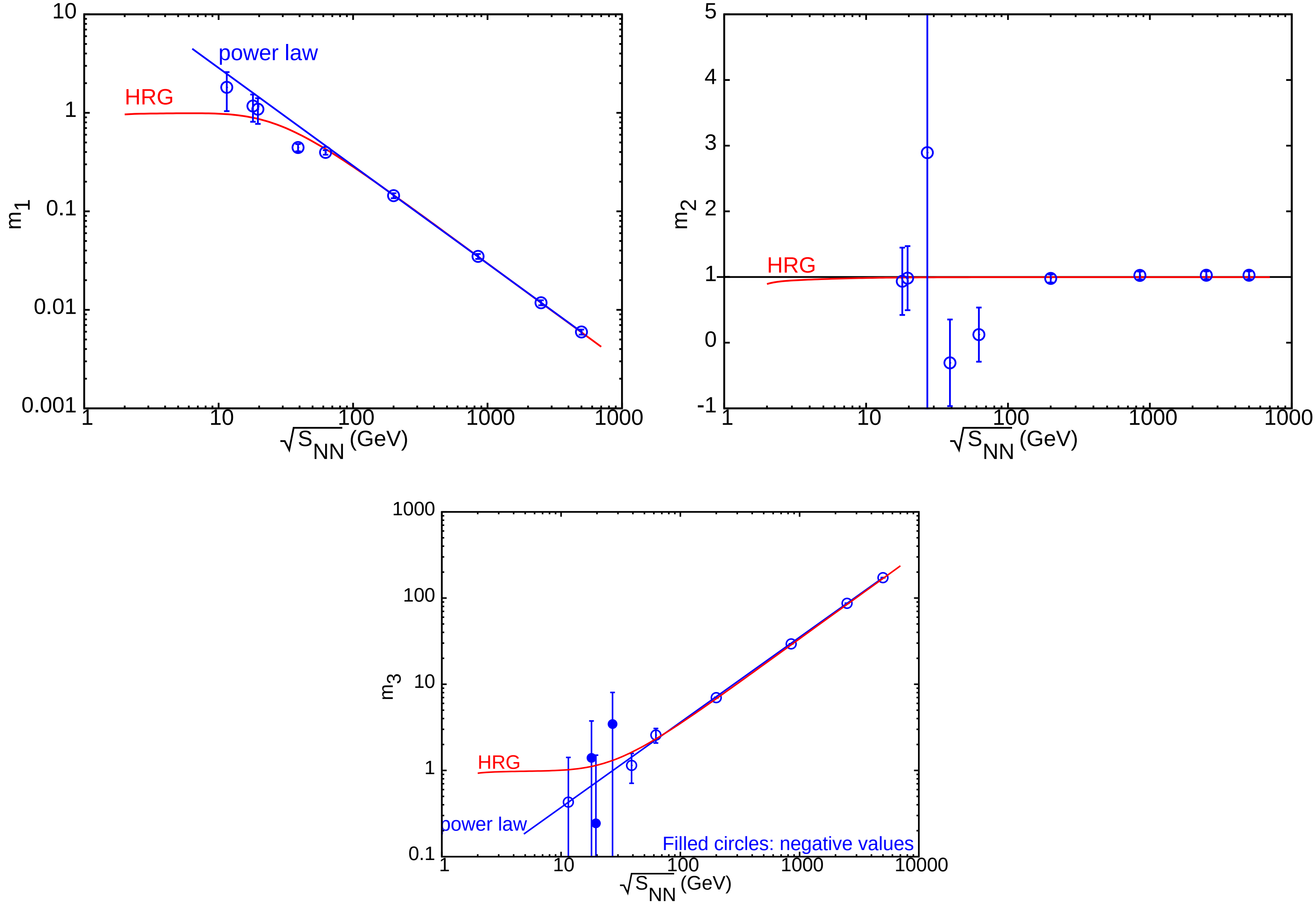

♠ Used $T_c(\mu = 0) = 170$ MeV (Gavai & Gupta, arXiv: 1001.3796).

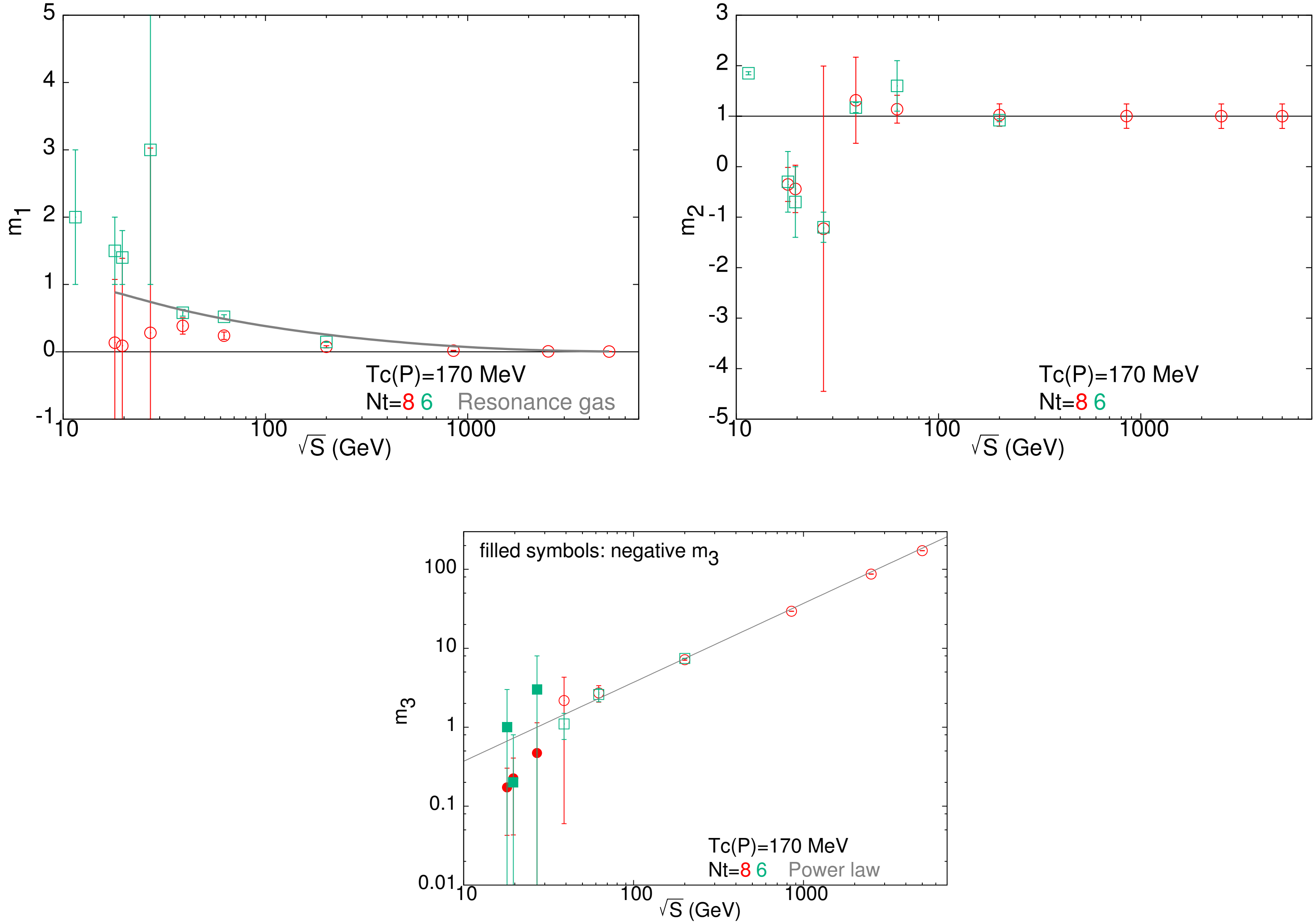

♠ Marginal change if $T_c = 175$ MeV (Datta, Gavai & Gupta, QM '12).

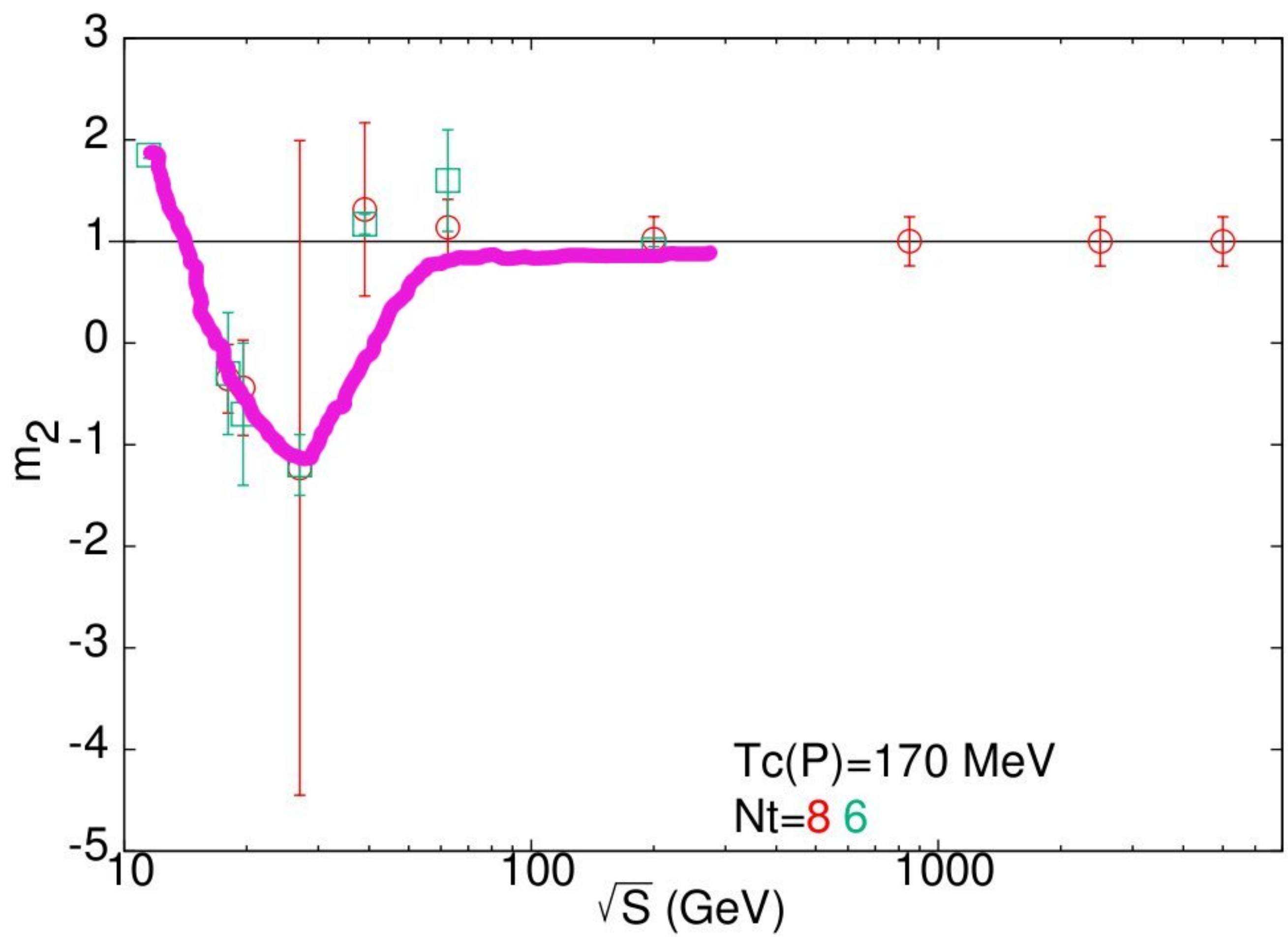

Gavai-Gupta, '10 & Datta-Gavai-Gupta, QM '12

- Smooth & monotonic behaviour for large $\sqrt{s}$: $m_1 \downarrow$ and $m_3 \uparrow$.

- Note that even in this smooth region, an experimental comparison is exciting : Direct Non-Perturbative test of QCD in hot and dense environment.

- Smooth & monotonic behaviour for large $\sqrt{s}$: $m_1 \downarrow$ and $m_3 \uparrow$.
- Note that even in this smooth region, an experimental comparison is exciting : Direct Non-Perturbative test of QCD in hot and dense environment.
- Our estimated critical point suggests non-monotonic behaviour in all m_i, which should be accessible to the low energy scan of RHIC BNL !

- Smooth & monotonic behaviour for large $\sqrt{s}$: $m_1 \downarrow$ and $m_3 \uparrow$.

- Note that even in this smooth region, an experimental comparison is exciting : Direct Non-Perturbative test of QCD in hot and dense environment.

- Our estimated critical point suggests non-monotonic behaviour in all m_i, which should be accessible to the low energy scan of RHIC BNL !

- Proton number fluctuations (Hatta-Stephenov, PRL 2003)

- Neat idea : directly linked to the baryonic susceptibility which ought to diverge at the critical point. Since diverging ξ is linked to σ mode, which cannot mix with any isospin modes, expect χ_I to be regular.

- Smooth & monotonic behaviour for large $\sqrt{s}$: $m_1 \downarrow$ and $m_3 \uparrow$.
- Note that even in this smooth region, an experimental comparison is exciting : Direct Non-Perturbative test of QCD in hot and dense environment.
- Our estimated critical point suggests non-monotonic behaviour in all m_i, which should be accessible to the low energy scan of RHIC BNL !
- Proton number fluctuations (Hatta-Stephenov, PRL 2003)
- Neat idea : directly linked to the baryonic susceptibility which ought to diverge at the critical point. Since diverging ξ is linked to σ mode, which cannot mix with any isospin modes, expect χ_I to be regular.
- Leads to a ratio χ_Q:χ_I:χ_B = 1:0:4
- Assuming protons, neutrons, pions to dominate, both χ_Q and χ_B can be shown to be proton number fluctuations only.

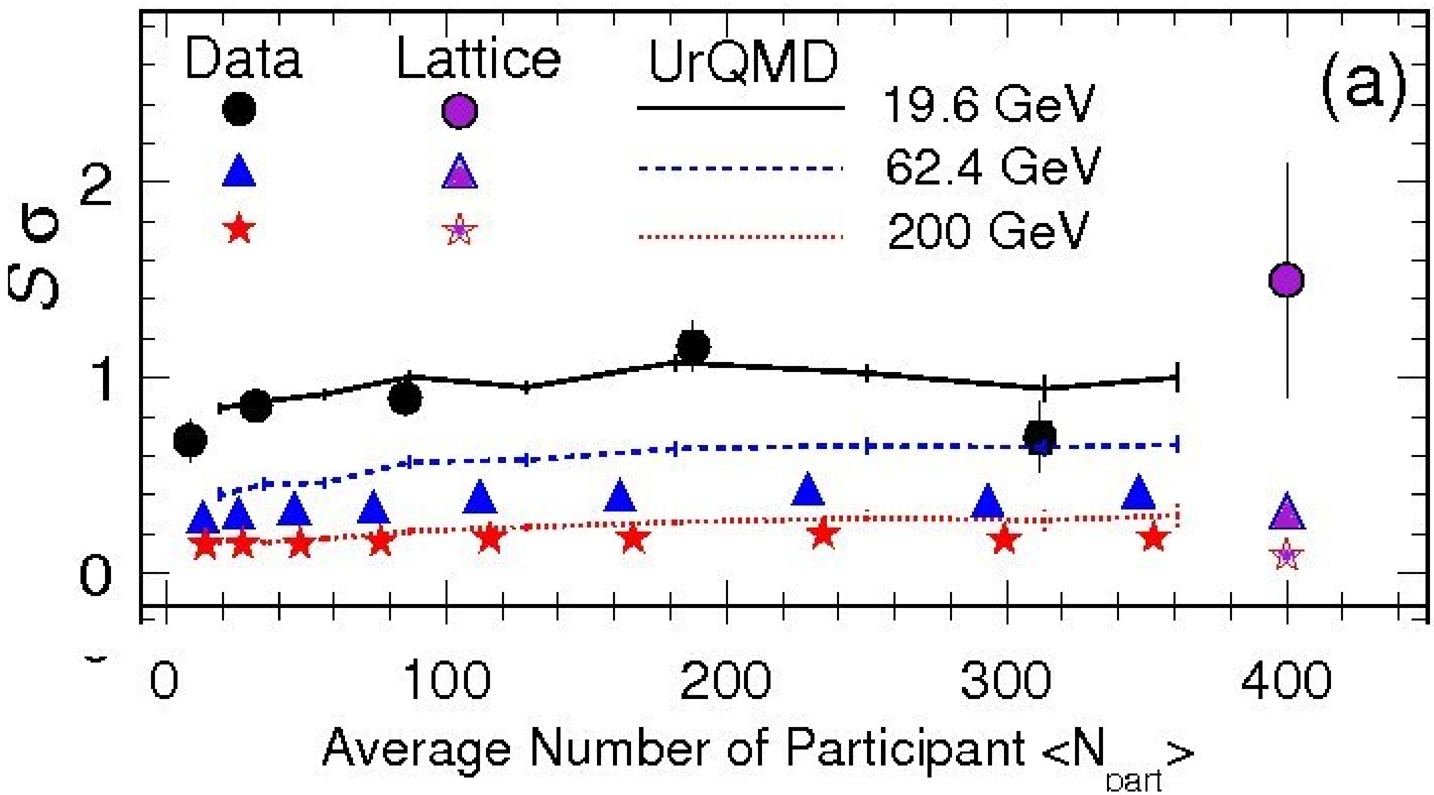

Aggarwal et al., STAR Collaboration, arXiv : 1004.4959

- Reasonable agreement with our lattice results. Where is the critical point ?

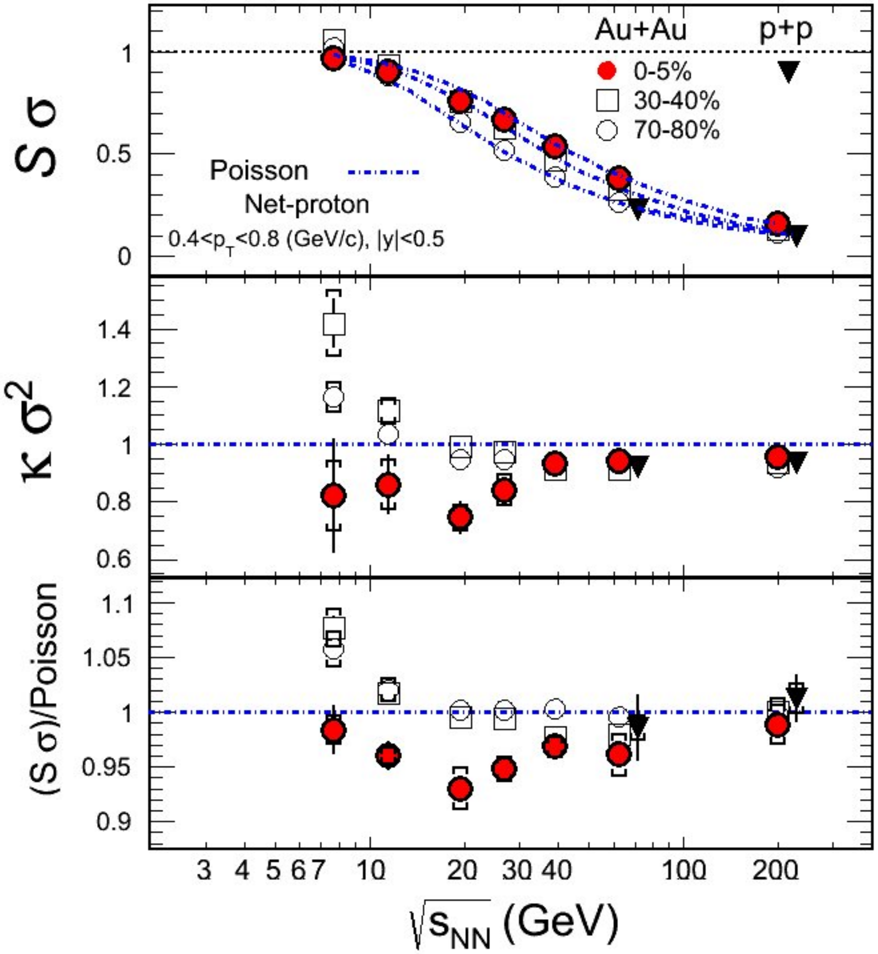

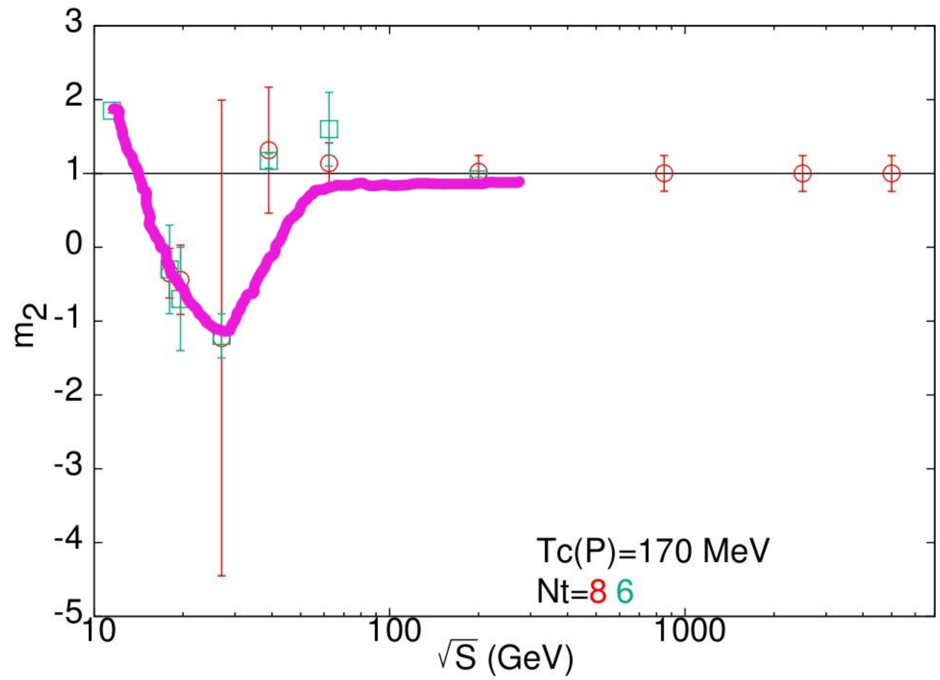

Xiaofeng Luo, QM'12
From STAR Collaboration

Gavai-Gupta, '10
Datta-Gavai-Gupta, QM '12

Summary

- Phase diagram in $T - \mu$ has begun to emerge: Different methods, $\rightsquigarrow$ similar qualitative picture. Critical Point at $\mu_B/T \sim 1 - 2$.

- Our results for $N_t = 8$ first to begin the inching towards continuum limit.

Summary

- Phase diagram in $T - \mu$ has begun to emerge: Different methods, $\rightsquigarrow$ similar qualitative picture. Critical Point at $\mu_B/T \sim 1 - 2$.

- Our results for $N_t = 8$ first to begin the inching towards continuum limit.

- We showed that Critical Point leads to structures in m_i on the Freeze-Out Curve. Possible Signatue ?

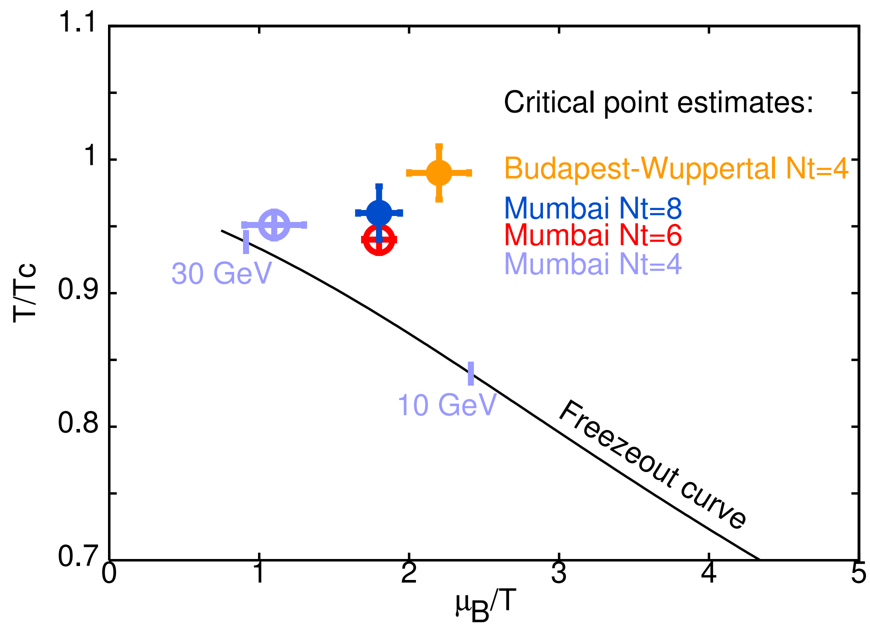

♡ STAR results appear to agree with our Lattice QCD predictions. ☺

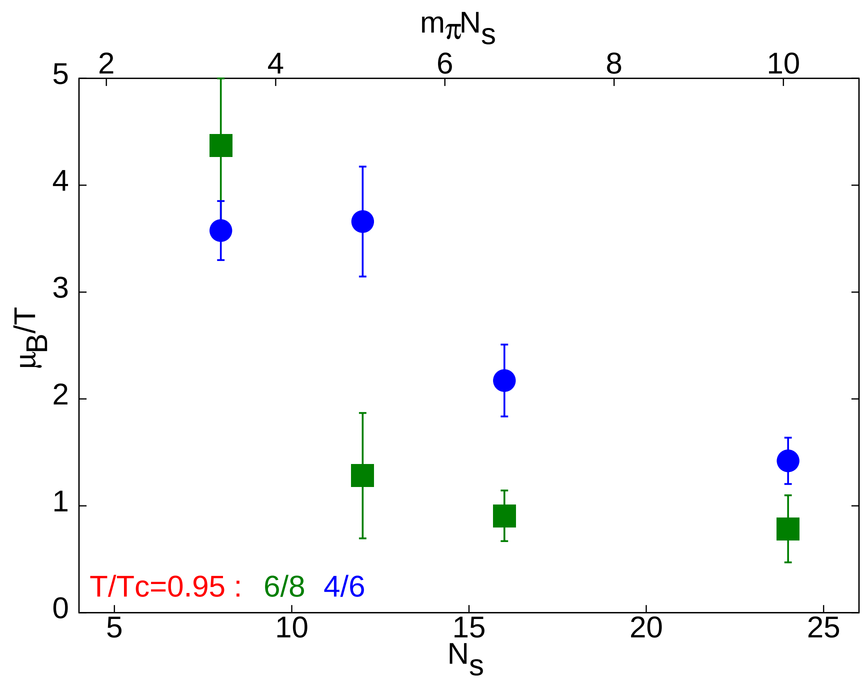

- Our estimate consistent with Fodor & Katz (2002) [$m_\pi/m_\rho = 0.31$ and $N_s m_\pi \sim$ 3-4].

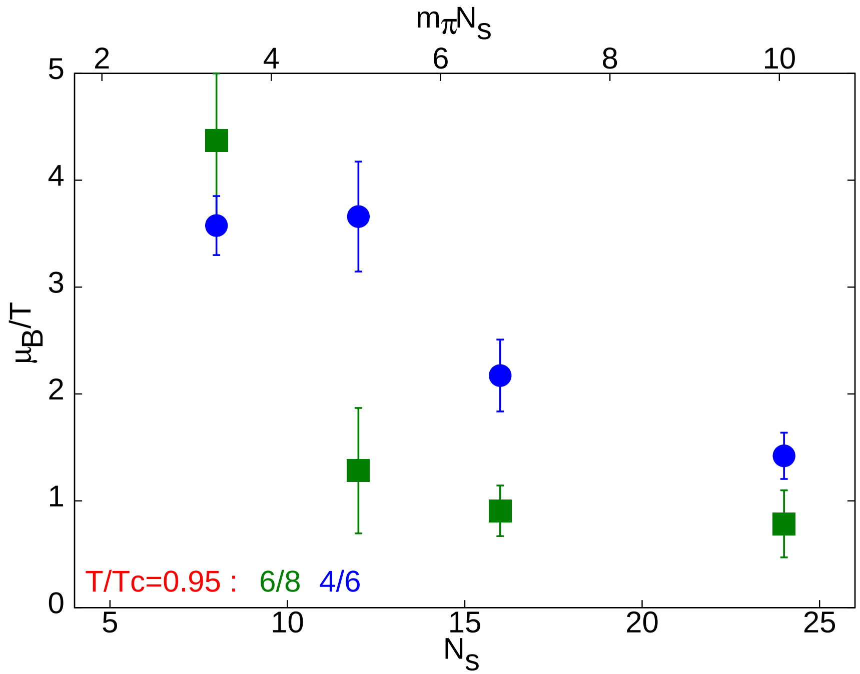

- Our estimate consistent with Fodor & Katz (2002) [$m_\pi/m_\rho = 0.31$ and $N_s m_\pi \sim$ 3-4].

- Strong finite size effects for small N_s. A strong change around $N_s m_\pi \sim 6$. (Compatible with arguments of Smilga & Leutwyler and also seen for hadron masses by Gupta & Ray)

The critical endpoint (II)

method for locating of the CEP:

- determine largest temperature where all coefficients are positive $\rightarrow T^{\mathrm{CEP}}$
- determine the radius of convergence at this temperature $\rightarrow \mu^{\mathrm{CEP}}$

$$p = c_0 + c_2\,(\mu_B/T)^2 + c_4\,(\mu_B/T)^4 + \cdots$$

$$\chi_B = 2c_2 + 12c_4\,(\mu_B/T)^2 + 30c_6\,(\mu_B/T)^4 + \cdots$$

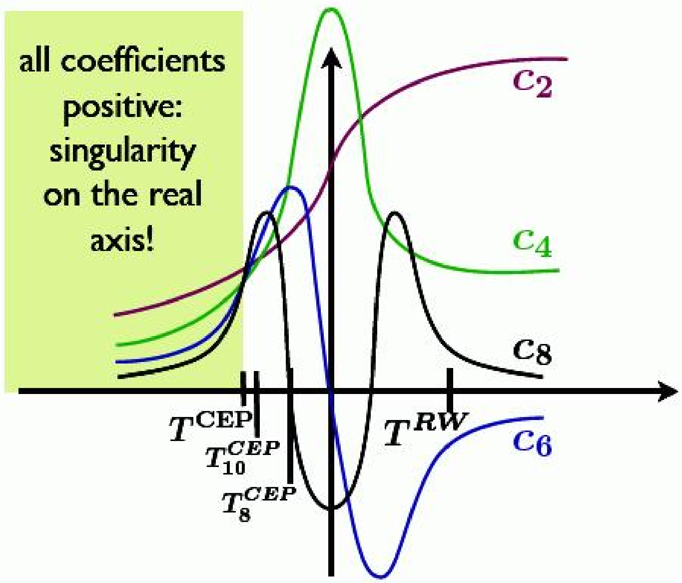

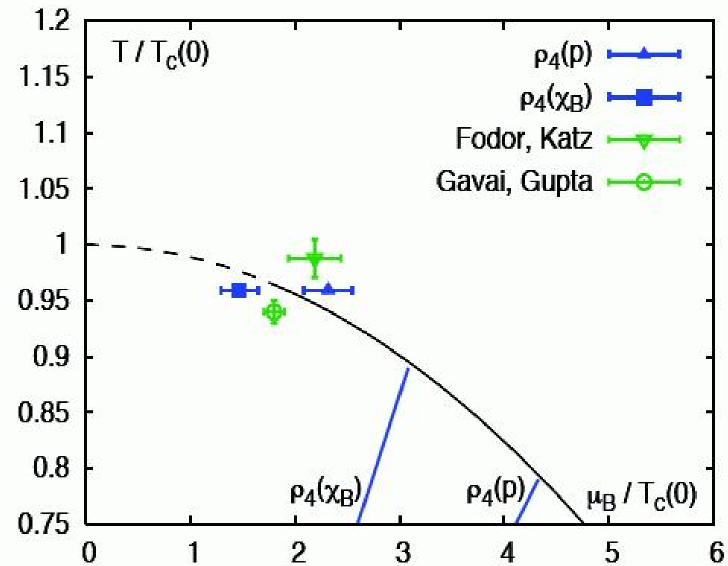

first non-trivial estimate of T^{CEP} by c_8
second non-trivial estimate of T^{CEP} by c_{10}

$$\rho_n(p) = \sqrt{c_n/c_{n+2}}$$

$$\rho = \lim_{n\to\infty} \rho_n$$

(Ch. Schmidt FAIR Lattice QCD Days, Nov 23-24, 2009.)

Imaginary Chemical Potential

deForcrand-Philpsen JHEP 0811

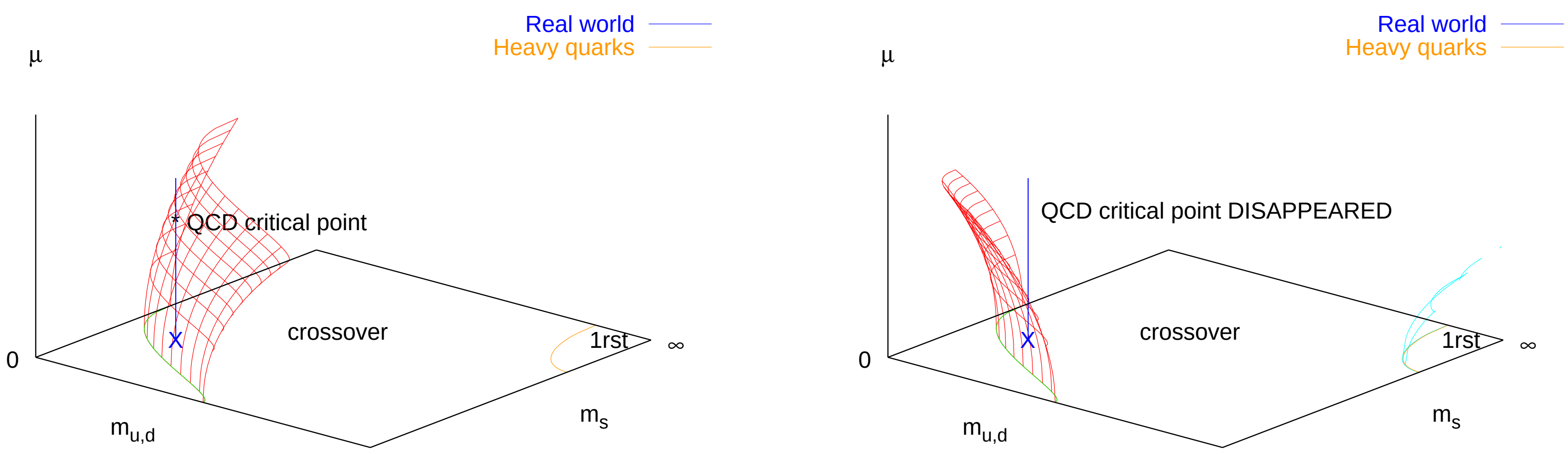

For $N_f = 3$, they find $\frac{m_c(\mu)}{m_c(0)} = 1 - 3.3(3)\left(\frac{\mu}{\pi T_c}\right)^2 - 47(20)\left(\frac{\mu}{\pi T_c}\right)^4$, i.e., m_c shrinks with μ.

Imaginary Chemical Potential

deForcrand-Philpsen JHEP 0811

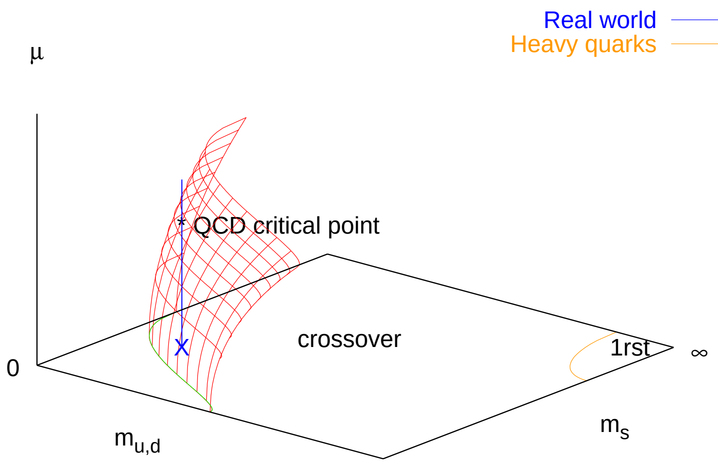

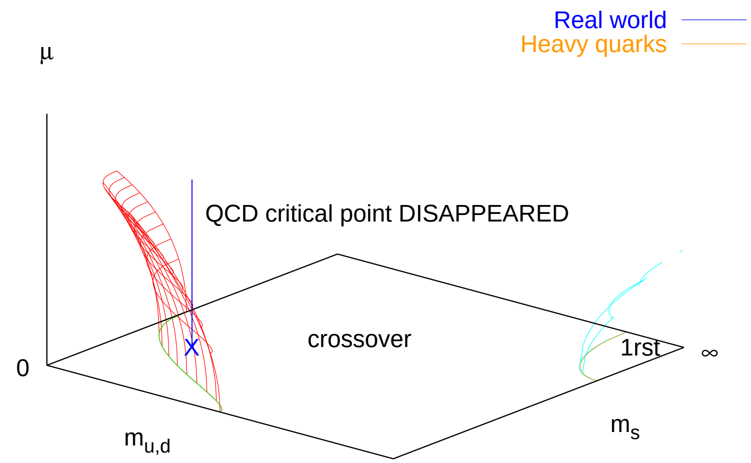

For $N_f = 3$, they find $\frac{m_c(\mu)}{m_c(0)} = 1 - 3.3(3)\left(\frac{\mu}{\pi T_c}\right)^2 - 47(20)\left(\frac{\mu}{\pi T_c}\right)^4$, i.e., m_c shrinks with μ.

Problems : i) Positive coefficient for finer lattice (Philipsen, CPOD 2009), ii) Known examples where shapes are different in real/imaginary μ, “The Critical line from imaginary to real baryonic chemical potentials in two-color QCD”, P. Cea, L. Cosmai, M. D’Elia, A. Papa, PR D77, 2008